Forward and Inverse Source Modeling

Zeynep AKALIN ACAR

12th EEGLAB Workshop, San Diego

November 19, 2010

Outline

- Basic definitions
- Forward model errors
- Example: epilepsy source localization

Source of Brain Electrical Activity

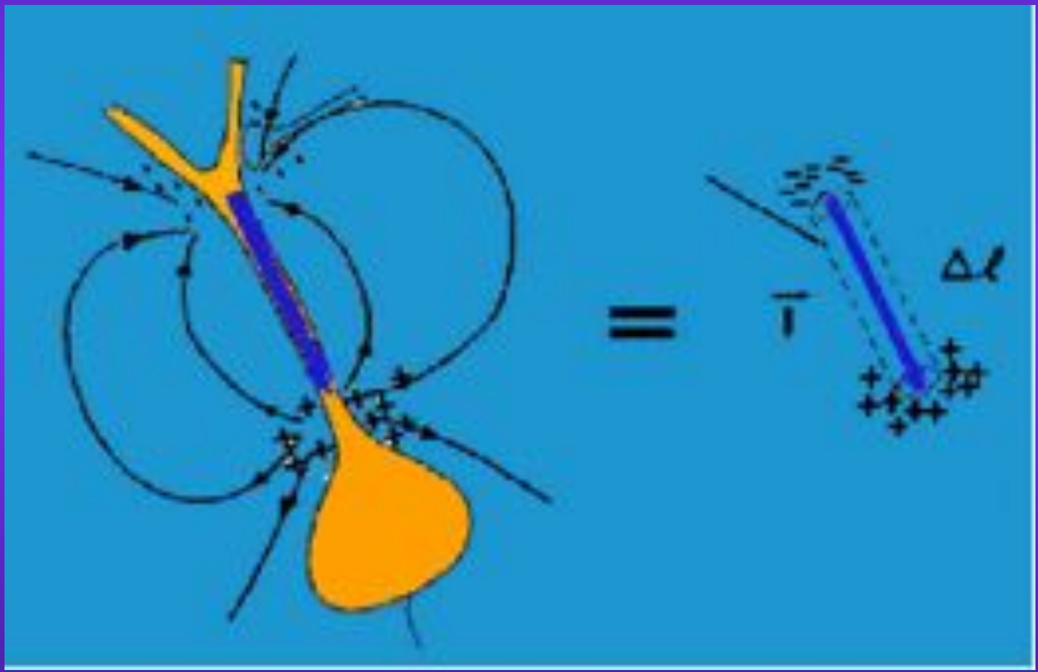

$$\vec{d} = \vec{I} \cdot \Delta l$$

Dipole ‘d’ is defined by is position and direction

Dipole representation of current sources

Potentials on the scalp

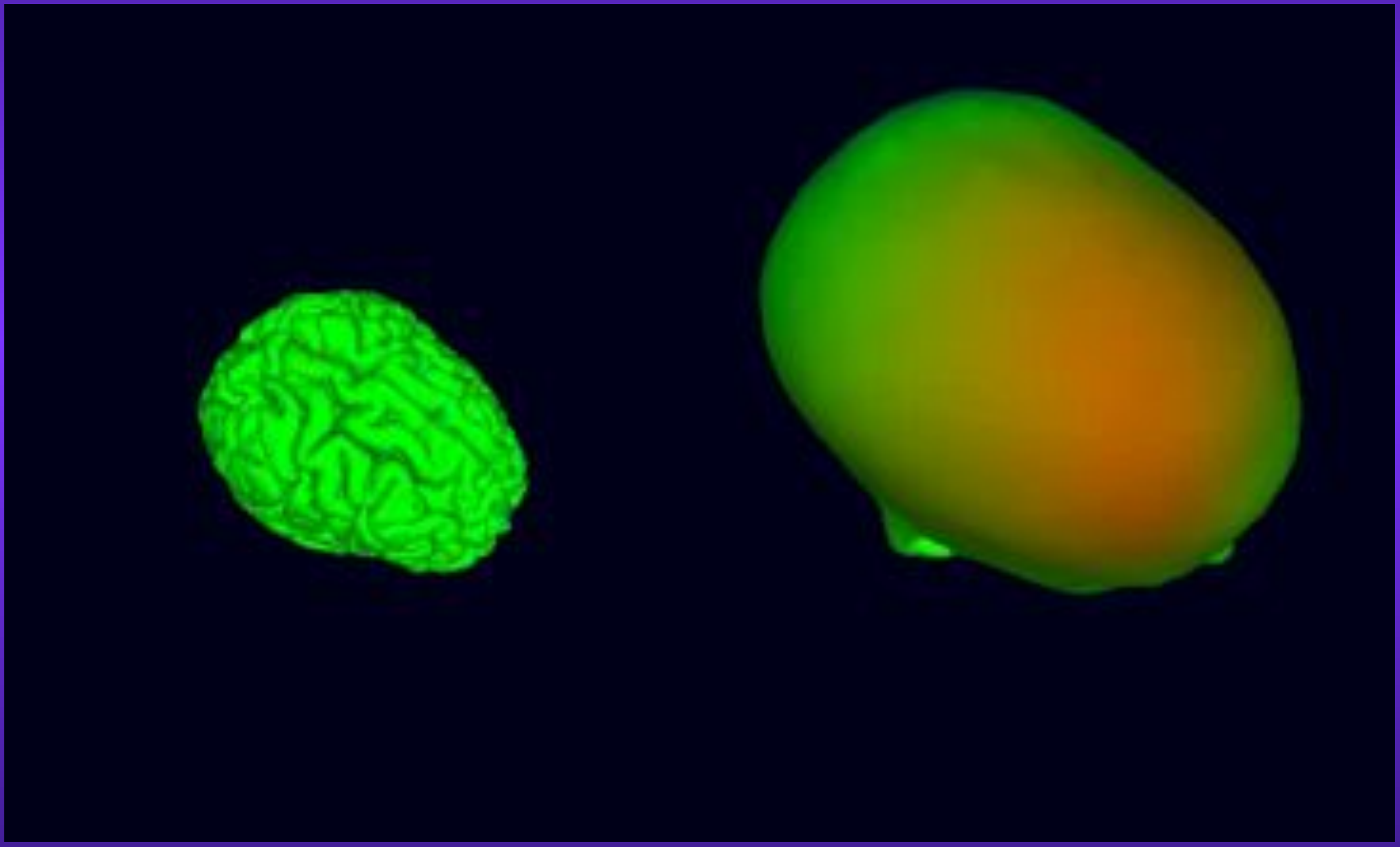

Forward and inverse problem

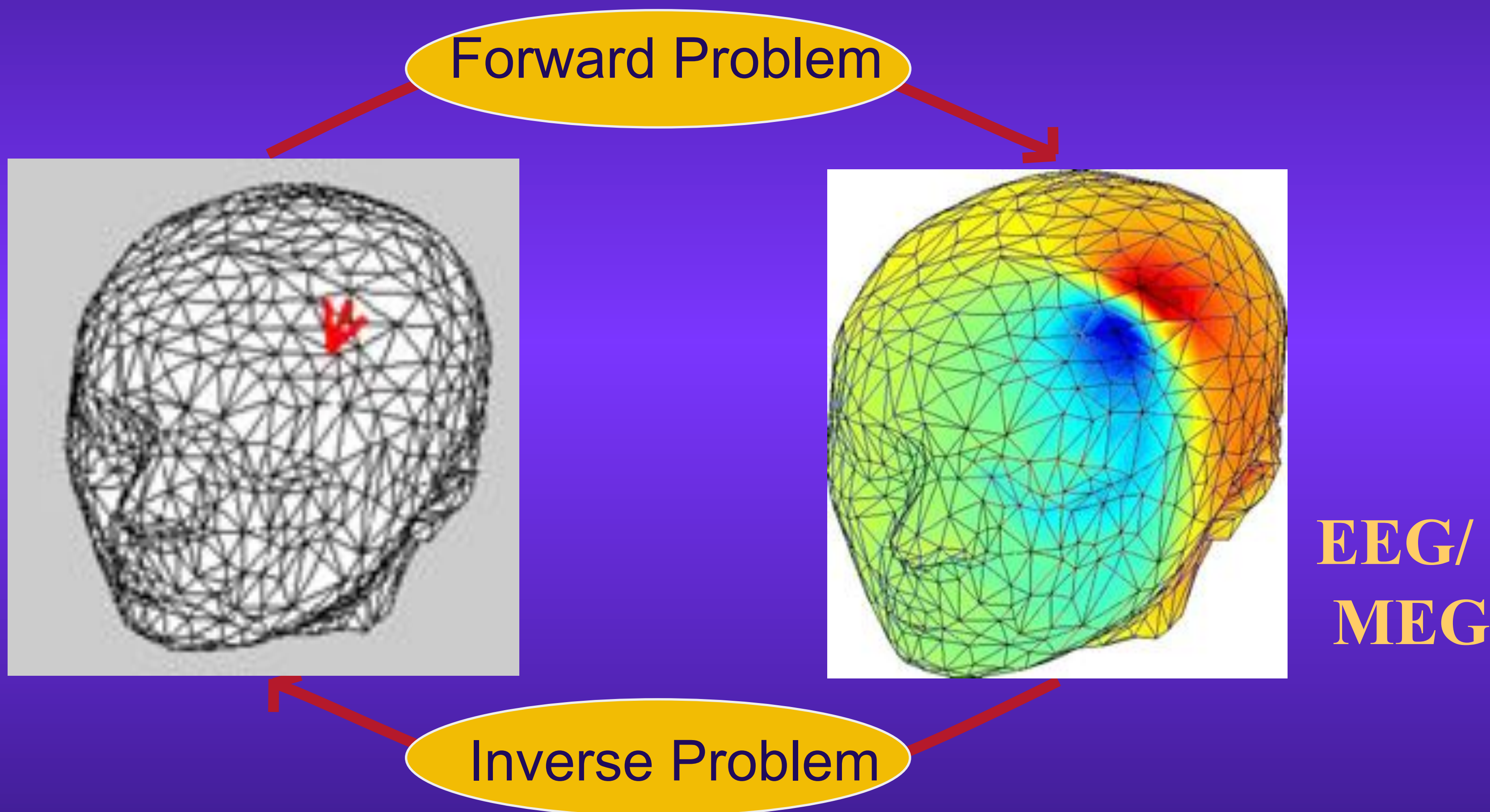

Infinite homogeneous medium

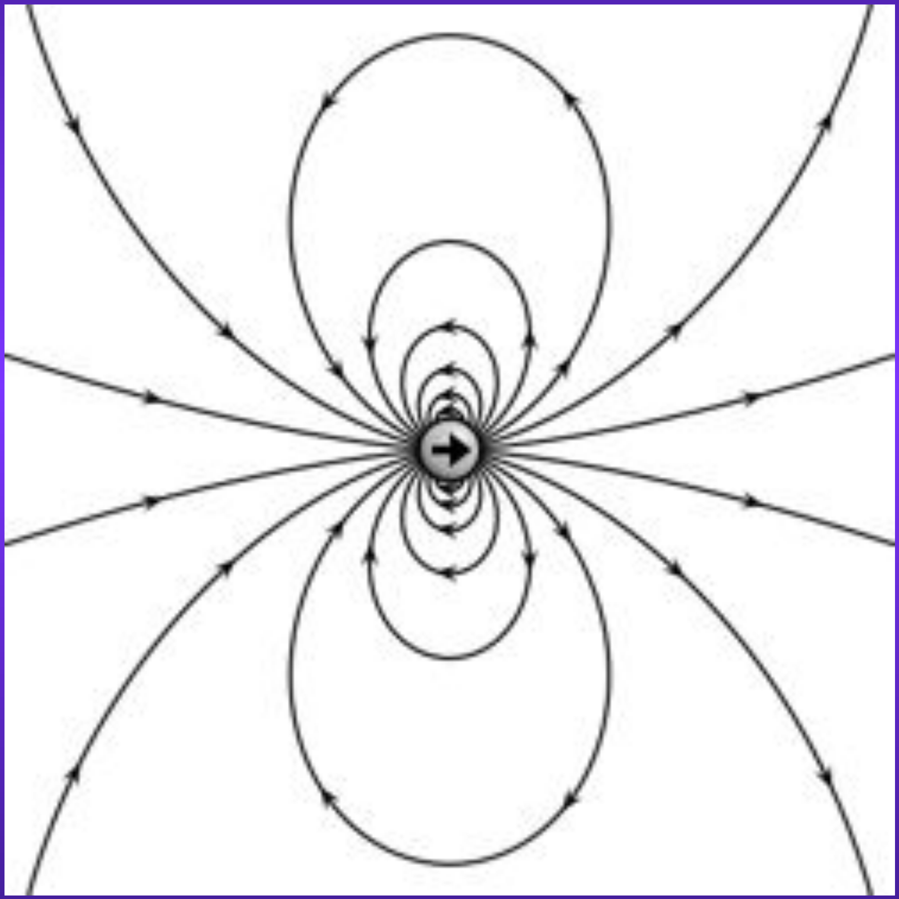

Field lines of a point dipole

$$\Phi(r) = \frac{1}{4\pi\varepsilon_o}\frac{\mathbf{p}\cdot\hat{\mathbf{r}}}{r^2}$$

Conducting homogeneous sphere

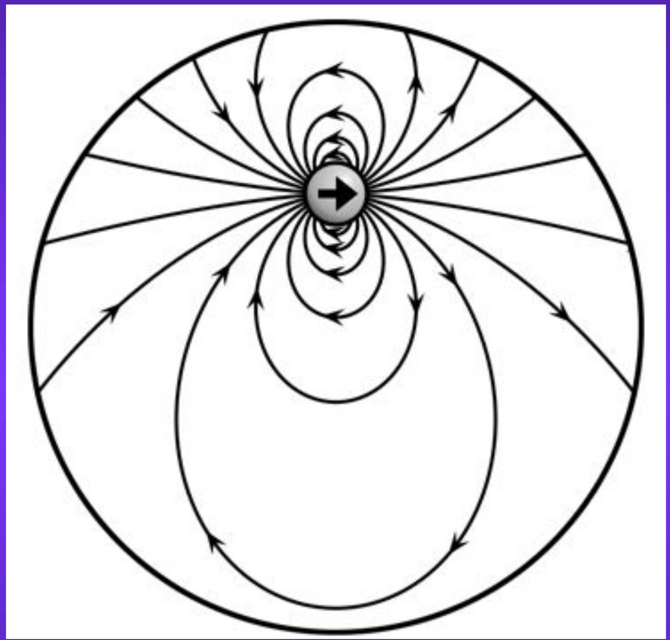

$$V = \frac{\vec{P}\cdot}{4\pi\sigma}\left\{2\frac{\vec{R}-\vec{r}_0}{r_p^3}+\frac{1}{R^2 r_p}\left[\vec{R}+\frac{\vec{R}r_0\ \cos\ \varphi - R\vec{r}_0}{R+r_p-r_0\ \cos\ \varphi}\right]\right\}$$

Surface potentials on a conducting homogeneous sphere

Multi-layer sphere

$$\Phi_b = \frac{I}{2\pi\sigma_t c}\sum_{n=1}^{\infty} A_n\left(\frac{r}{c}\right)^n\left[P_n(\cos\theta_A) - P_n(\cos\theta_B)\right]$$

$$\Phi_s = \frac{I}{2\pi\sigma_t c}\sum_{n=1}^{\infty}\left[S_n r^n + U_n r^{-(n+1)}\right] \cdot\left[P_n(\cos\theta_A) - P_n(\cos\theta_B)\right]$$

$$\Phi_t = \frac{I}{2\pi\sigma_t c}\sum_{n=1}^{\infty}\left[T_n r^n + W_n r^{-(n+1)}\right] \cdot\left[P_n(\cos\theta_A) - P_n(\cos\theta_B)\right].$$

$$A_n = \frac{(2n+1)^3/2n}{\begin{aligned}\Big\{&\left[\left(\frac{\sigma_b}{\sigma_s}+1\right)n+1\right]\left[\left(\frac{\sigma_s}{\sigma_t}+1\right)n+1\right] \\ &+\left(\frac{\sigma_b}{\sigma_s}-1\right)\left(\frac{\sigma_s}{\sigma_t}-1\right)n(n+1)\left(\frac{a}{b}\right)^{2n+1} \\ &+\left(\frac{\sigma_s}{\sigma_t}-1\right)(n+1)\left[\left(\frac{\sigma_b}{\sigma_s}+1\right)n+1\right]\left(\frac{b}{c}\right)^{2n+1} \\ &+\left(\frac{\sigma_b}{\sigma_s}-1\right)(n+1)\left[\left(\frac{\sigma_s}{\sigma_t}+1\right)(n+1)-1\right]\left(\frac{a}{c}\right)^{2n+1}\Big\}\end{aligned}}$$

(where σ_b, σ_s, and σ_t are the conductivities of the three regions)

$$S_n = \frac{\frac{A_n}{c^n}\left[\left(1-\frac{\sigma_b}{\sigma_s}\right)n+1\right]}{2n+1}$$

$$U_n = \frac{\frac{A_n}{c^n}n\left(1-\frac{\sigma_b}{\sigma_s}\right)a^{2n+1}}{2n+1}$$

$$T_n = \frac{A_n}{c^n(2n+1)^2}\left\{\left[\left(1+\frac{\sigma_b}{\sigma_s}\right)n+1\right]\left[\left(1+\frac{\sigma_s}{\sigma_t}\right)n+1\right]+n(n+1)\left(1-\frac{\sigma_b}{\sigma_s}\right)\left(1-\frac{\sigma_s}{\sigma_t}\right)\left(\frac{a}{b}\right)^{2n+1}\right\}$$

$$W_n = \frac{nA_n}{c^n(2n+1)^2}\left\{\left(1-\frac{\sigma_s}{\sigma_t}\right)\left[\left(1+\frac{\sigma_b}{\sigma_s}\right)n+1\right]b^{2n+1}+\left(1-\frac{\sigma_b}{\sigma_s}\right)\left[\left(1+\frac{\sigma_s}{\sigma_t}\right)n+\frac{\sigma_s}{\sigma_t}\right]a^{2n+1}\right\}.$$

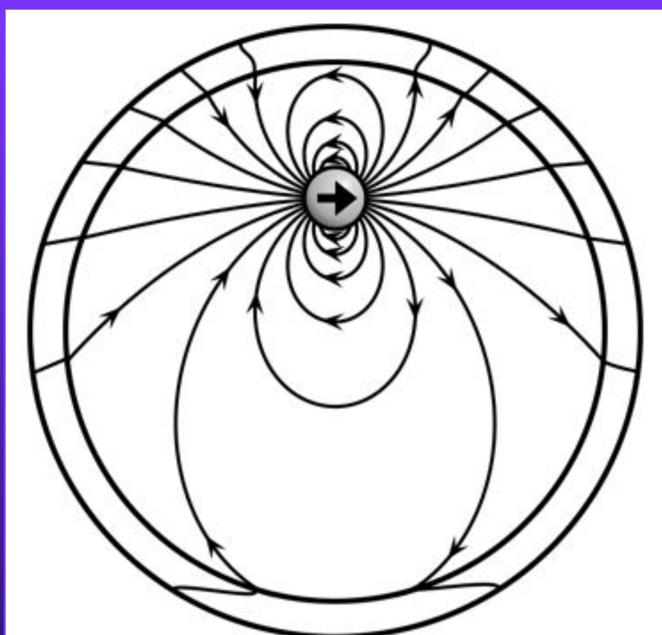

Concentric conducting spheres
[Rush and Driscoll, 1969]

Analytical Head Models

- Spheroid
- Homogeneous Sphere
- Multi-Layer Sphere
  - 3-Layer: Scalp, Skull, Brain
  - 4-Layer: Scalp, Skull, CSF, Brain

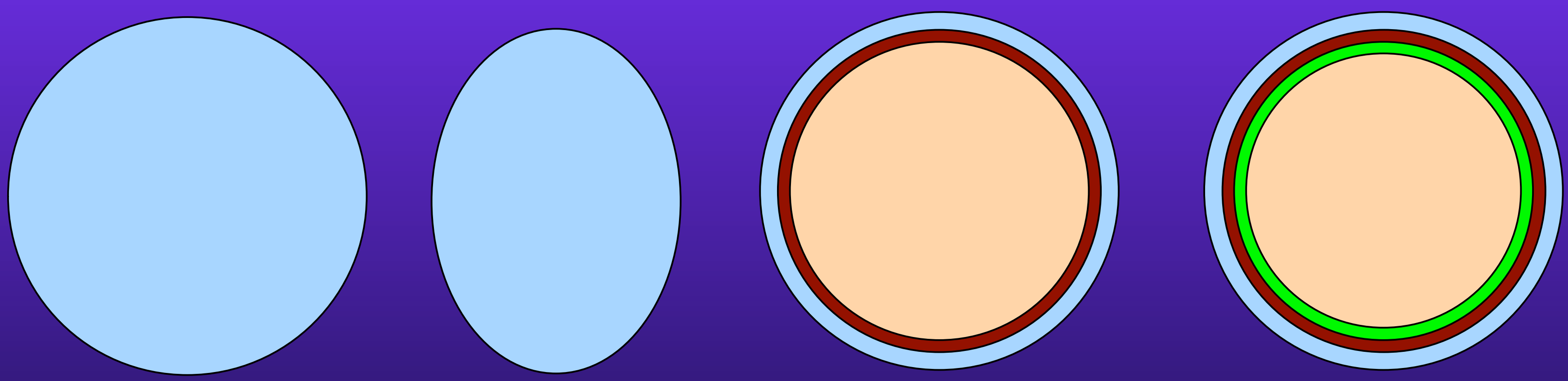

Human head

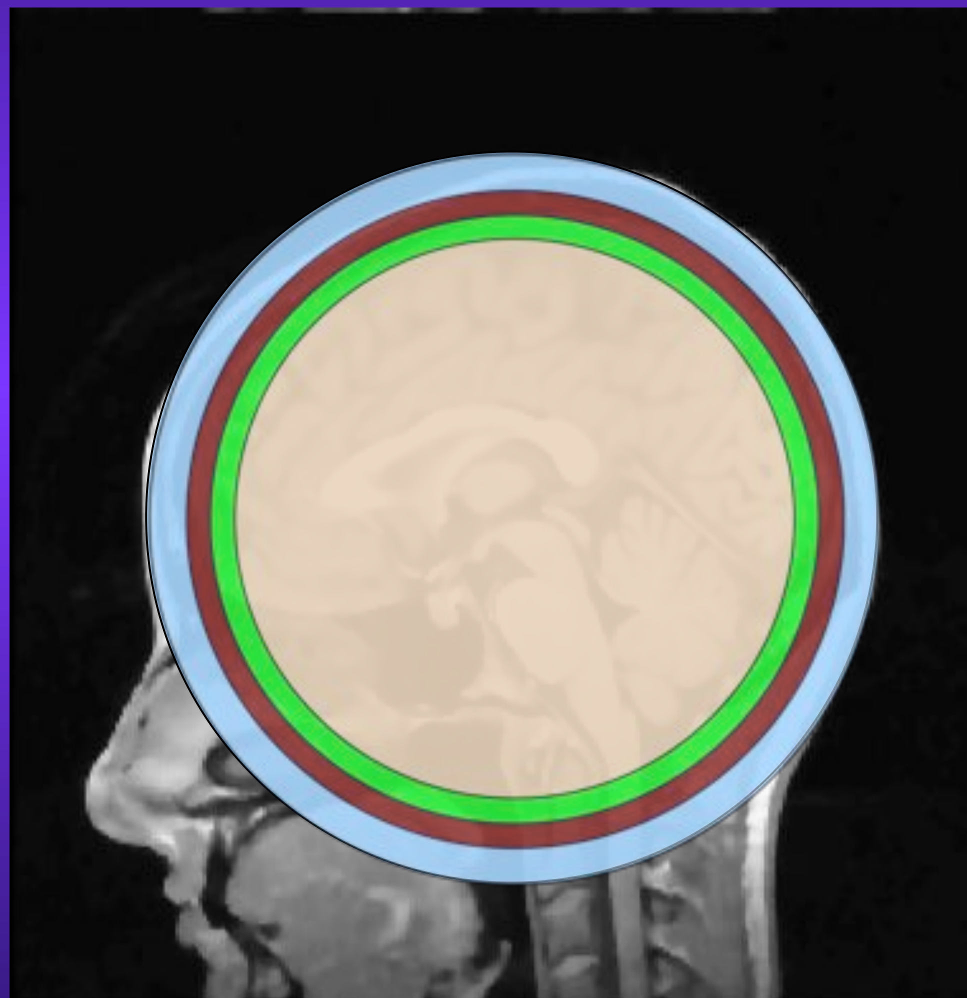

Numerical methods

- Boundary Element Method (BEM)
- Finite Element Method (FEM)
- Finite Difference Method (FDM)

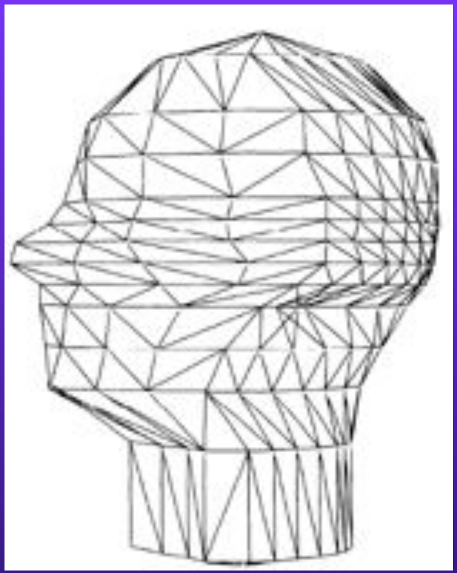

Meijs et al, 1989

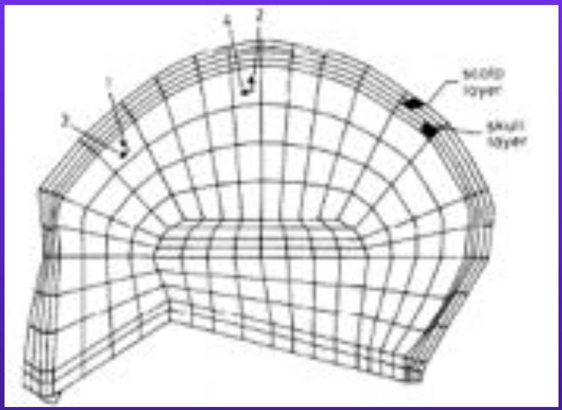

Yan et al, 1991

Formulation

Integral equation for Potential Field:

$$\phi(\vec{r}) = 2g(\vec{r}) + \frac{1}{2\pi}\sum_{k=1}^{n}\left(\frac{\sigma_k^- - \sigma_k^+}{\sigma_i^- - \sigma_i^+}\right)\int_{S_k}\phi(\vec{r}\,')\frac{\vec{R}}{R^3}\cdot d\vec{S}_k(\vec{r}\,')$$

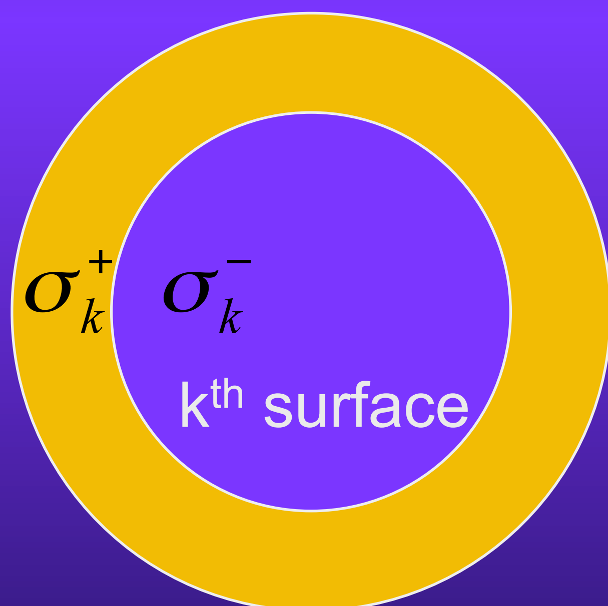

Formulation

Integrating the previous integral equation over all elements a set of equations are obtained.

In matrix notation for the potential field we obtain

$$\Phi_{M\times 1} = C_{M\times M}\Phi + g_{M\times 1} \qquad \Phi = [I - C]^{-1} g \qquad \Phi = \mathbf{A}^{-1} g$$

M: number of nodes

The expression for the magnetic field:

$$B_{n\times 1} = B_0 + \mathbf{H}_{n\times M}\Phi$$

n: number of magnetic sensors

Numerical Head Models

BEM

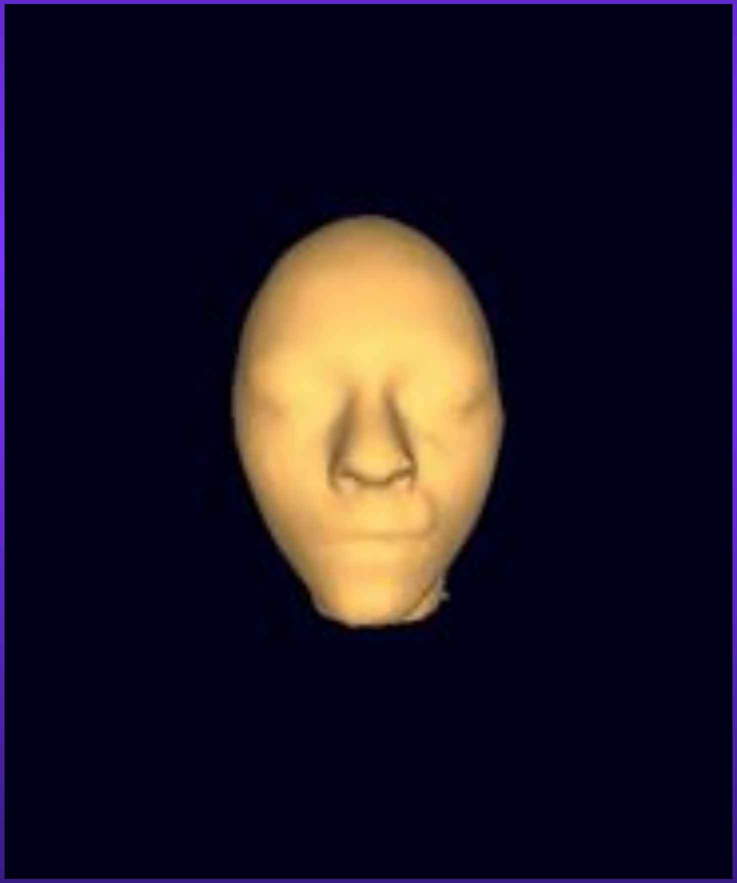

NFT BEM mesh

FEM

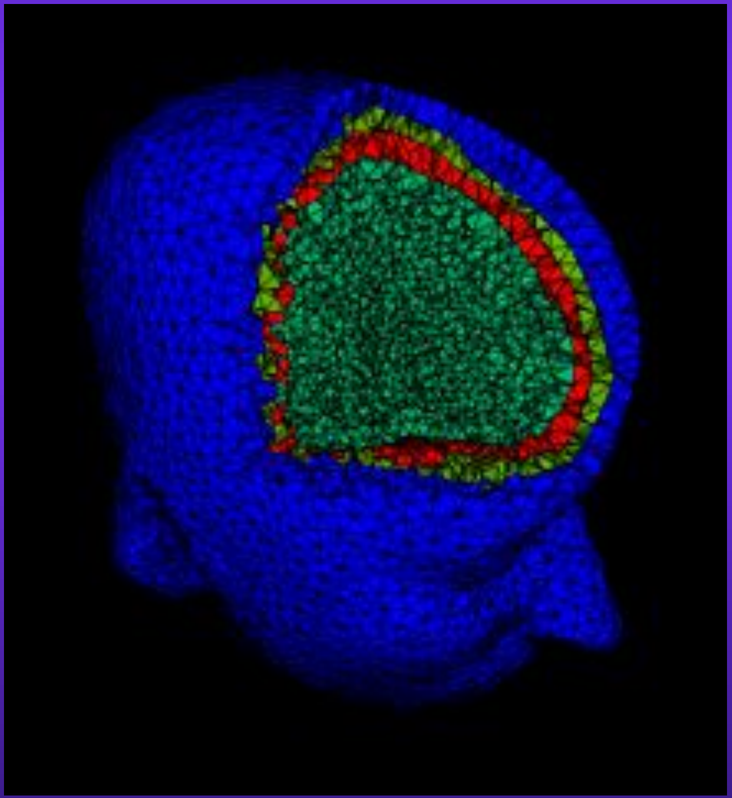

Generated using Tetgen
from NFT BEM mesh

FEM/BEM comparison

	BEM	FEM
Position of computational points	surface	volume
Free choice of computational points	yes	yes
System matrix	full	sparse
Solvers	direct	iterative
Number of compartments	small	large
Requires tesselation	yes	yes
Handles anisotropy	no	yes

Source models

Equivalent current dipole

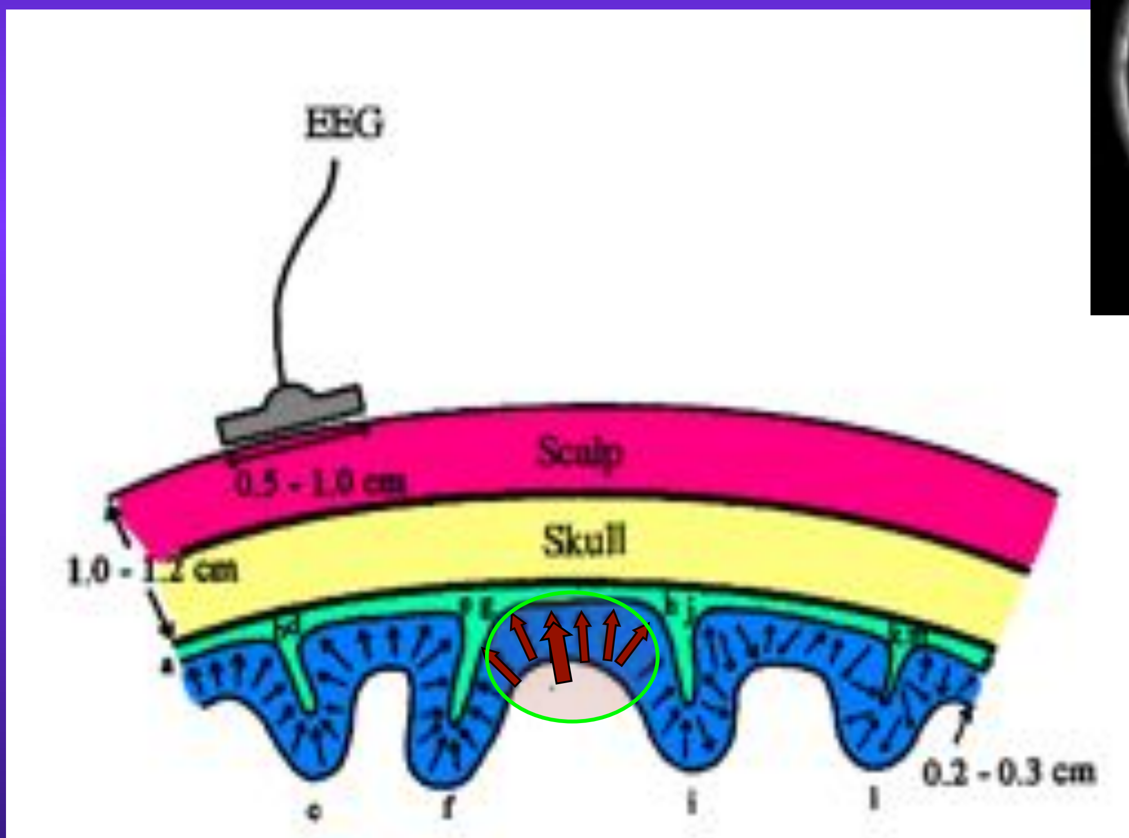

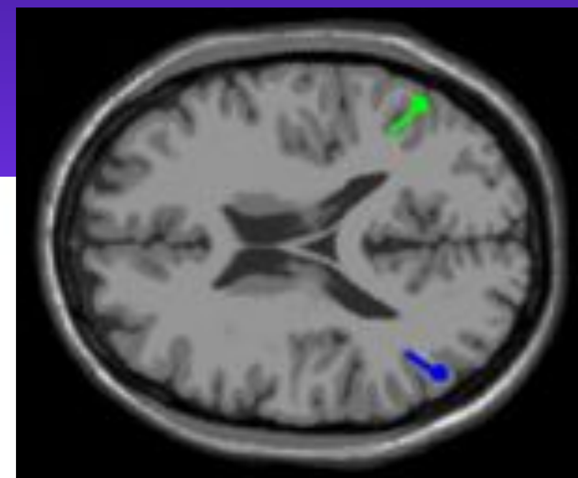

Overdetermined
Nonlinear optimization

Source space:
Brain volume

Source models

Distributed source models

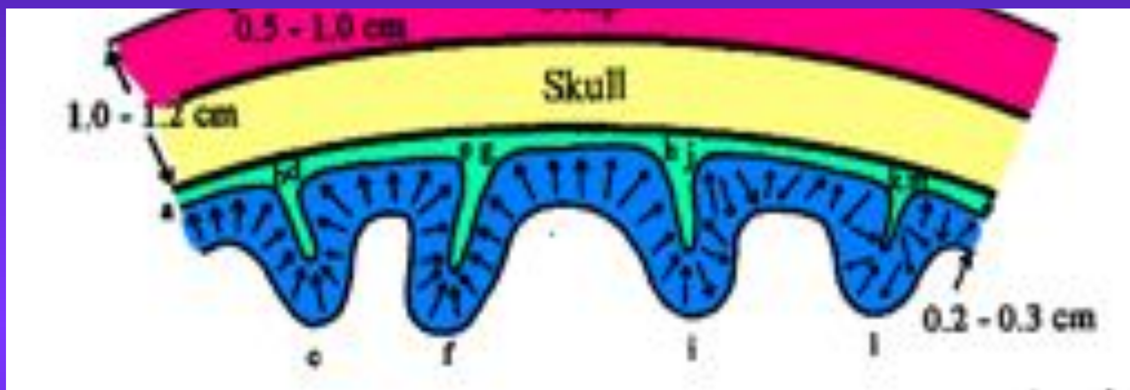

Source space:
Cortical surface

Overlapping patches

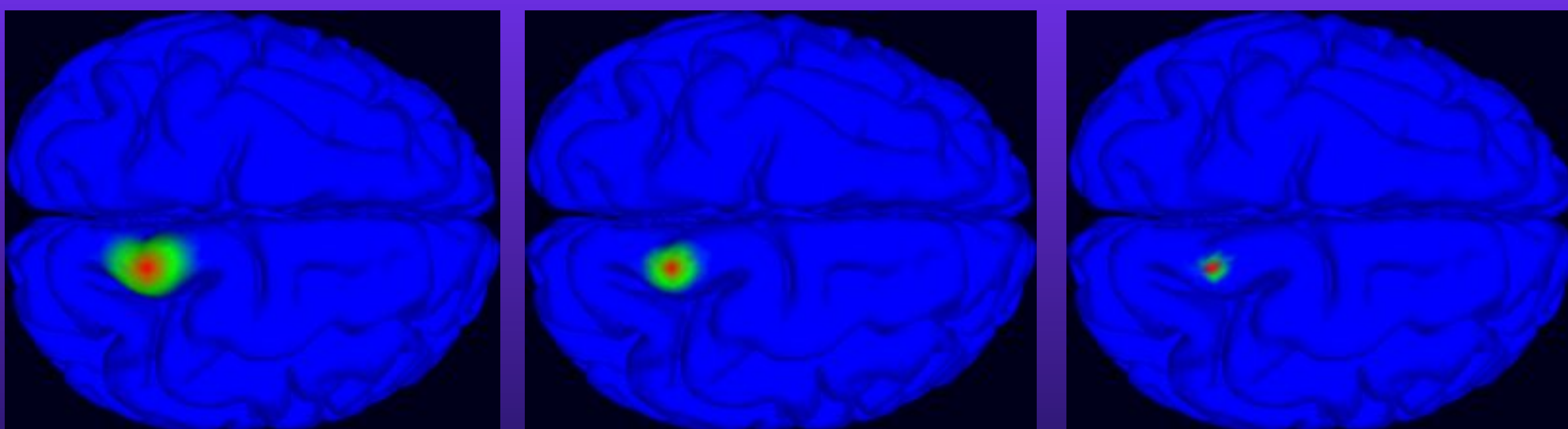

Inverse Problem

Parametric Methods

- Overdetermined
- Searches for parameters of a number of dipoles
- Nonlinear optimization techniques
- May converge to local minima

Imaging Methods

- Underdetermined
- Searches for activation in given locations.
- Linear optimization techniques
- Needs additional constraints

Effects of Forward Model Errors on EEG Source Localization

MODELING ERRORS

Head Model Generation

- Reference Head Model
  - From whole head T1 weighted MR of subject
  - 4-layer realistic BEM model
- MNI Head model
  - From the MNI head
  - 3-layer and 4-layer template BEM model
- Warped MNI Head Model
  - Warp MNI template to EEG sensors
- Spherical Head model
  - 4-layer concentric spheres
  - Fitted to EEG sensor locations

The Reference Head Model

- 18541 nodes
- 37090 elements
  - 6928 Scalp
  - 6914 Skull
  - 11764 CSF
  - 11484 Brain

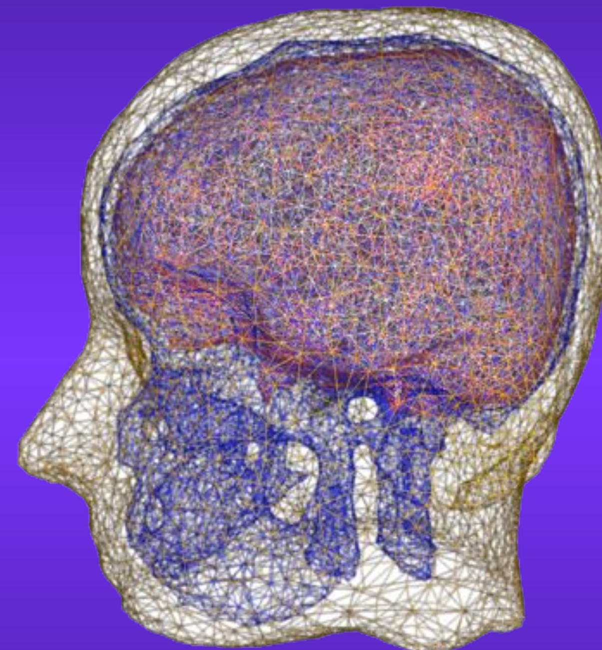

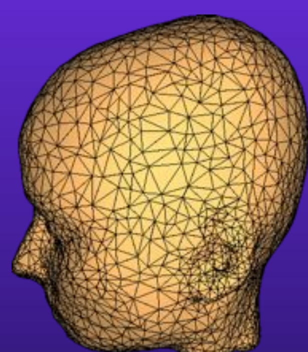

Scalp

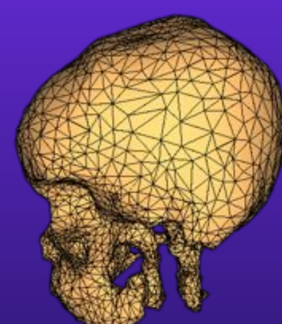

Skull

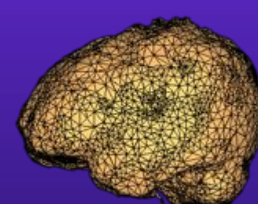

CSF

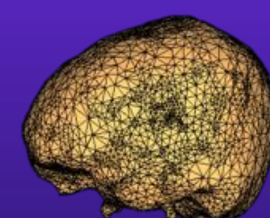

Brain

The MNI Head Model

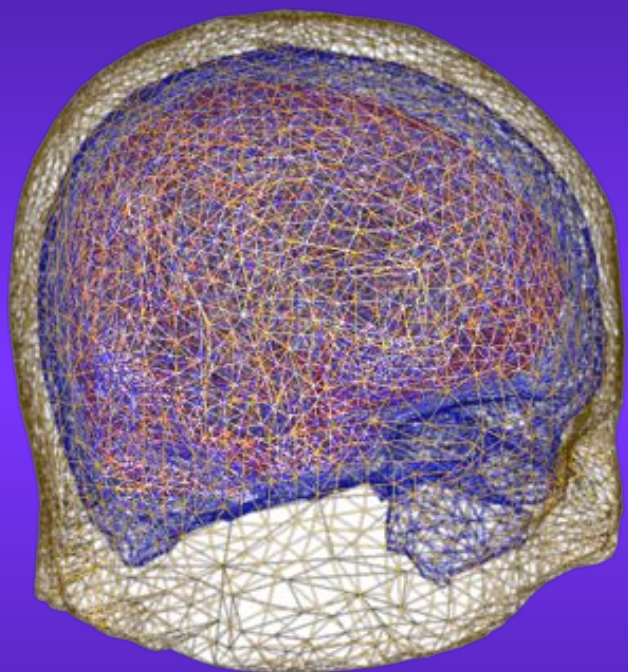

- 4-layer
  - 16856 nodes
  - 33696 elements
- 3-layer
  - 12730 nodes
  - 25448 elements

Brain

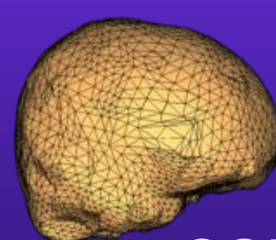

CSF

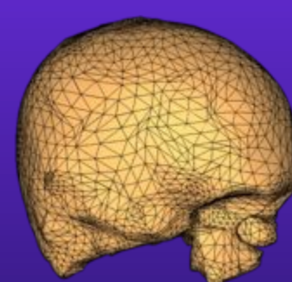

Skull

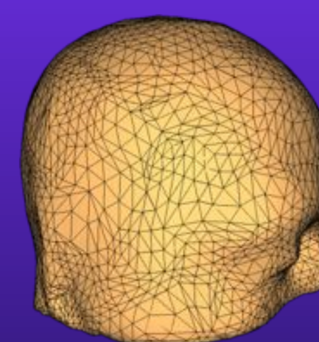

Scalp

The Warped MNI Head Model

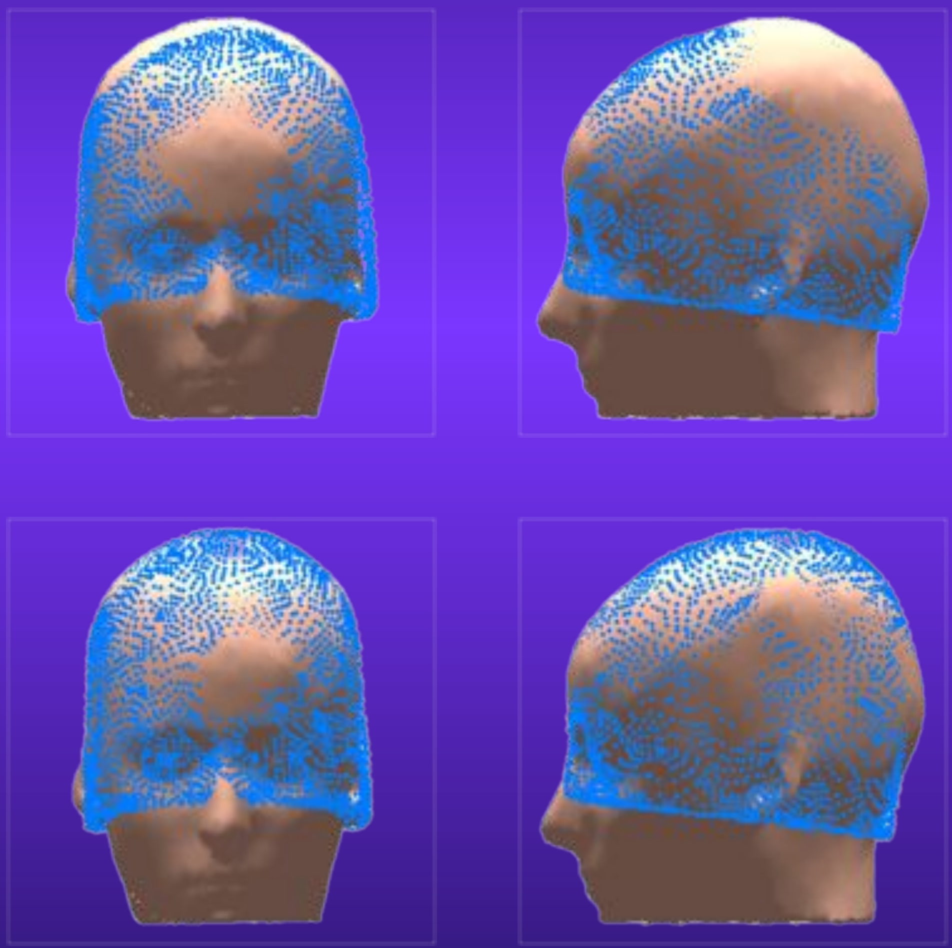

Registered MNI template

Warped MNI mesh

The Spherical Head Model

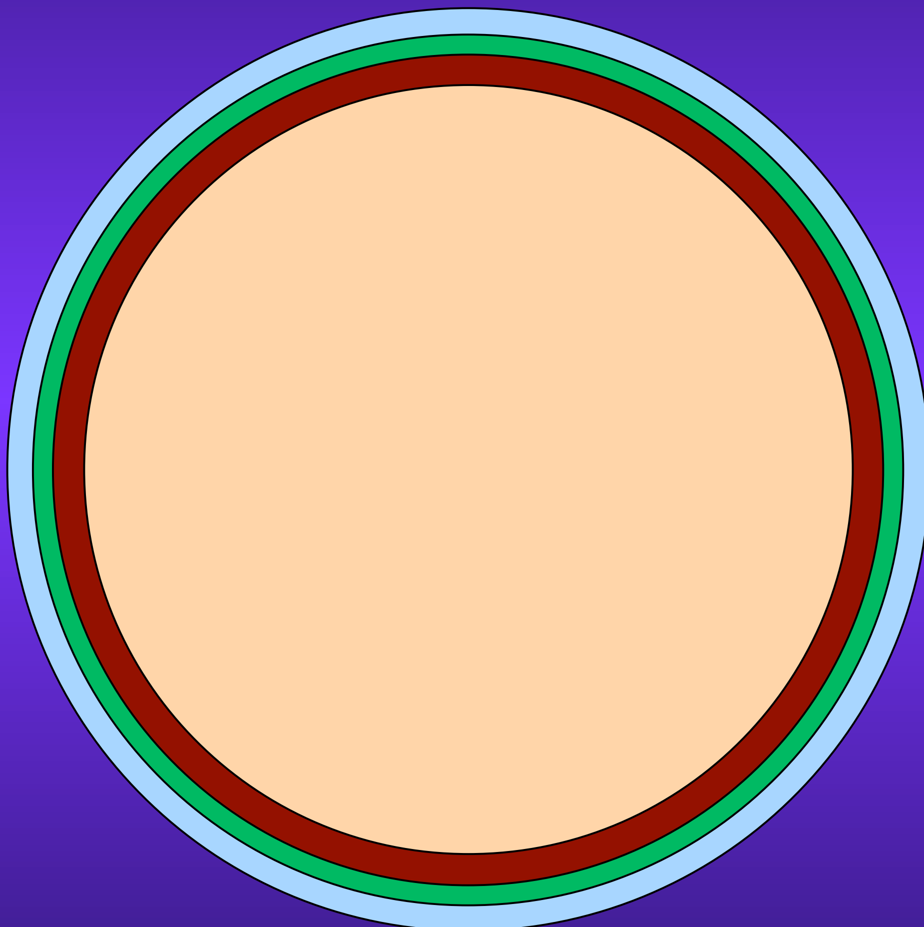

4-Layer model
Outer layer is fitted to electrode positions

Forward Problem Solution

BEM mesh → **BEM Matrix Generator** → BEM Matrices
Model param. →

BEM Matrices → **Invert Sensor Columns** → Transfer Matrices
Sensor locations →

[# of sensors x # of nodes]

Transfer Matrices → **Generate RHS, Multiply** → Lead Field Matrix
Dipole Field →

[# of sensors x # of dipoles]

Head Modeling Errors

- Solve FP with reference model
  - 3D grid inside the brain.
  - 3 Orthogonal dipoles at each point
  - 6,717 dipoles total
- Localize using other head models
  - Single dipole search.
- Plot location and orientation errors

Spherical Model Location Errors

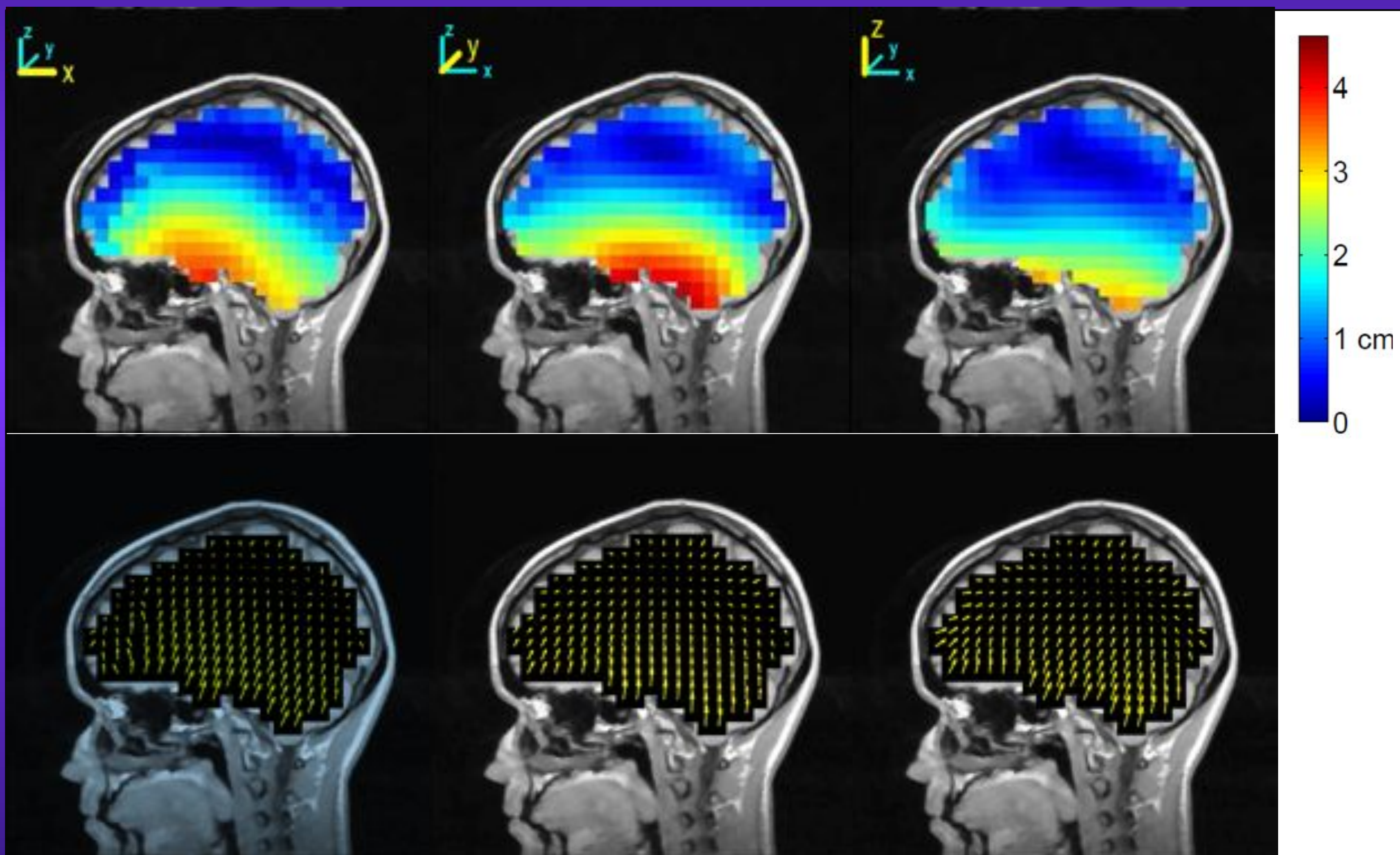

Spherical Model Direction Errors

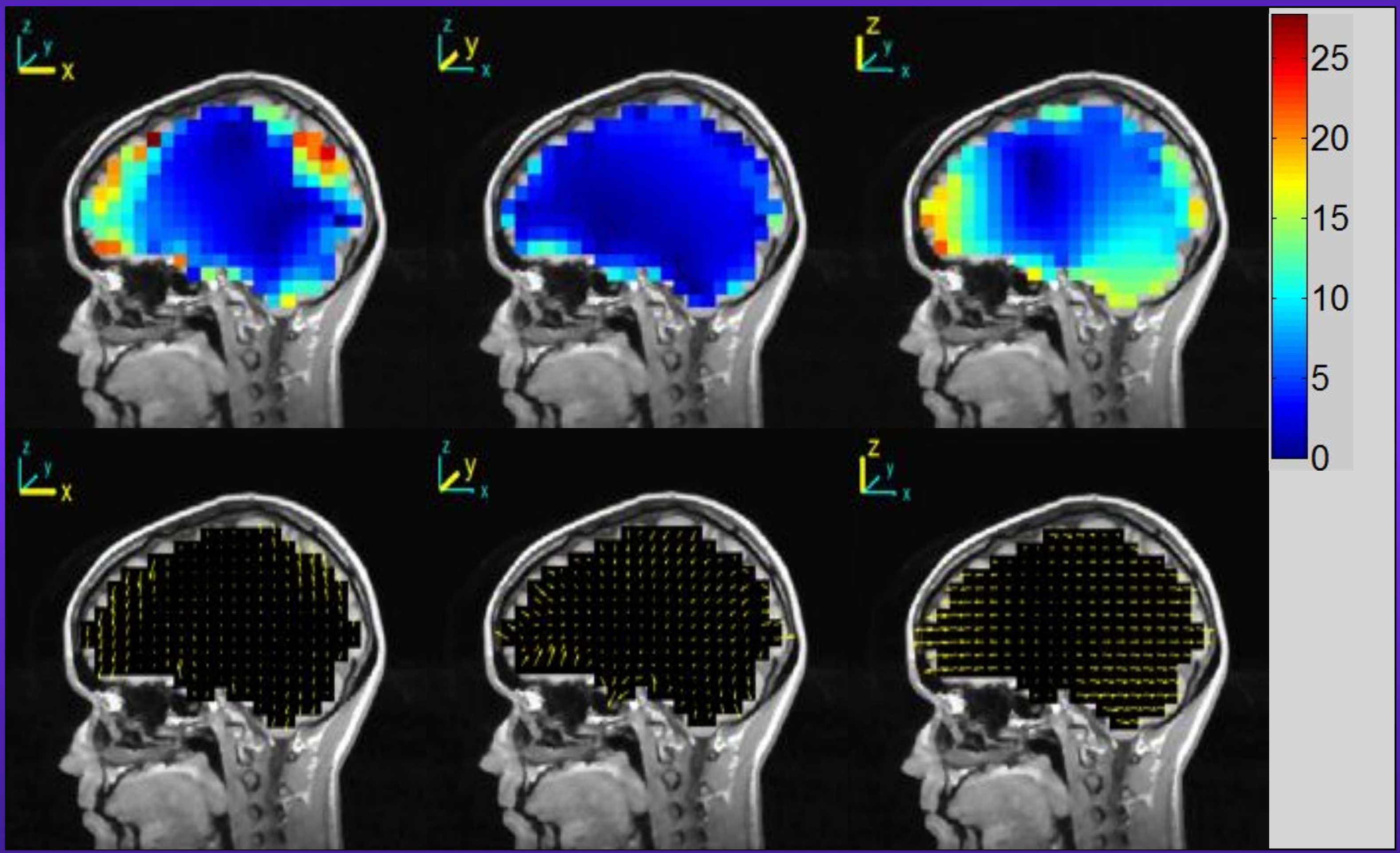

3-Layer MNI Location Errors

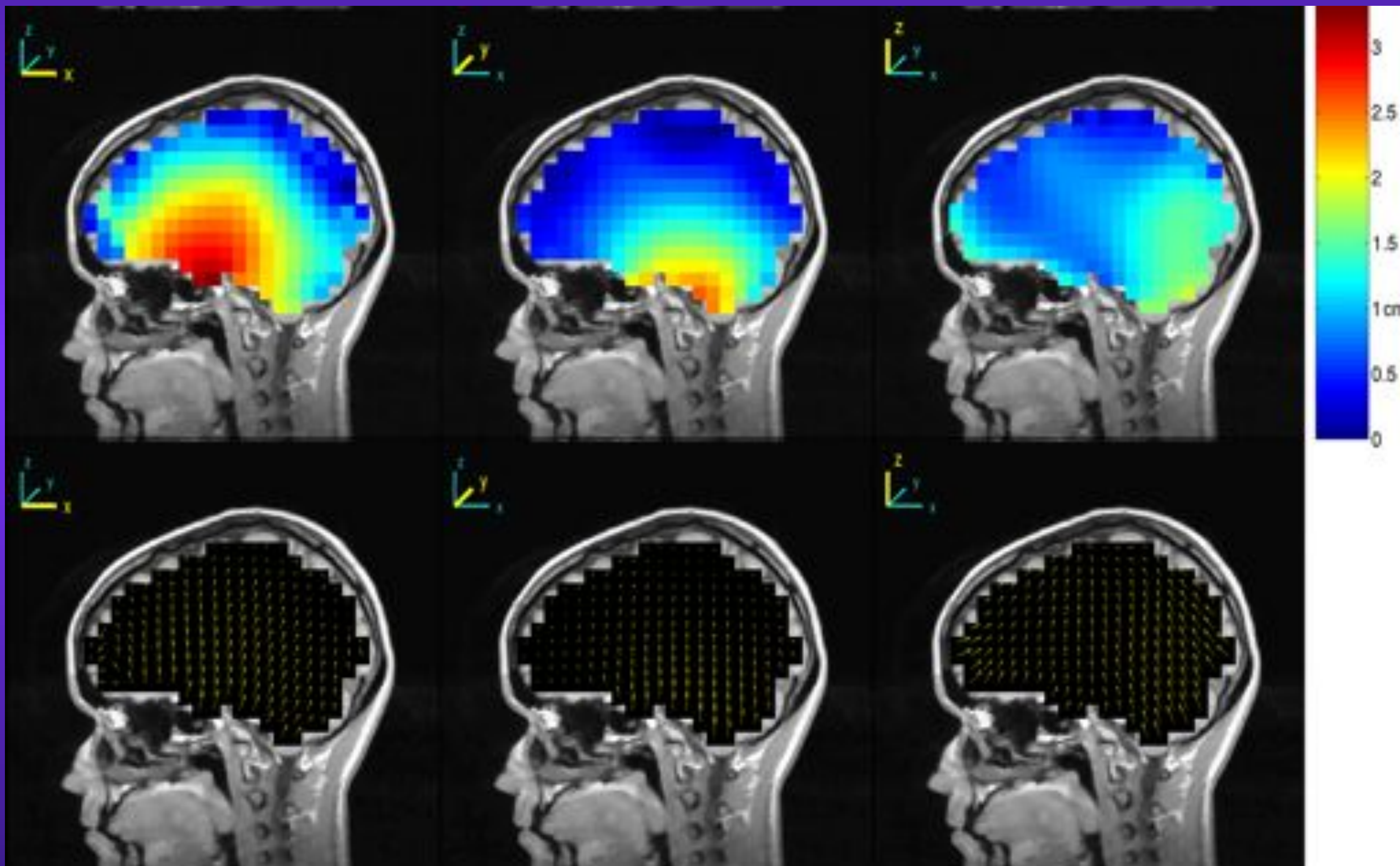

3-Layer MNI Direction Errors

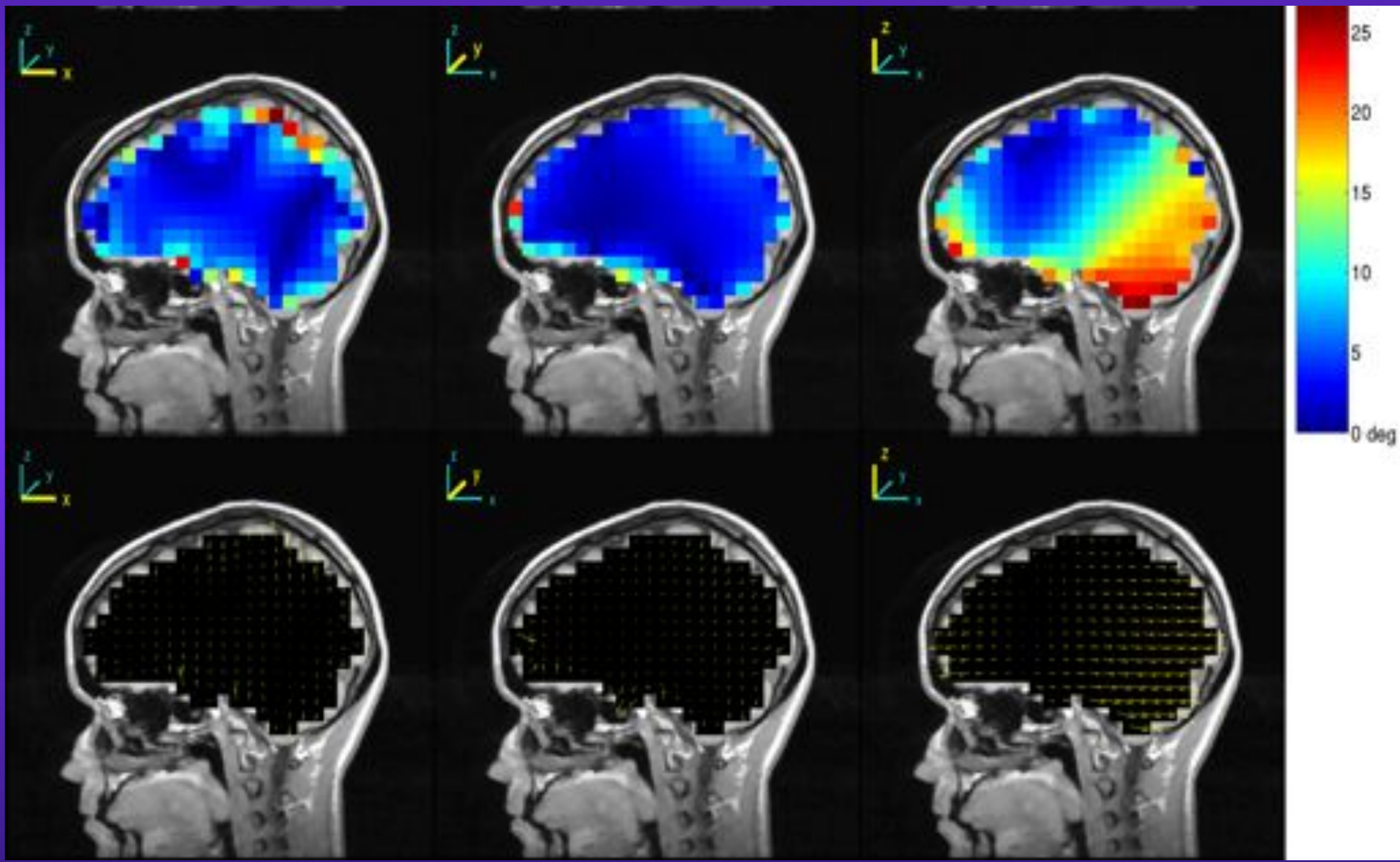

Source localization errors of patch activity

Forward Problem
Source : patches of cortex

Reference head model:
4-layer MR-based BEM

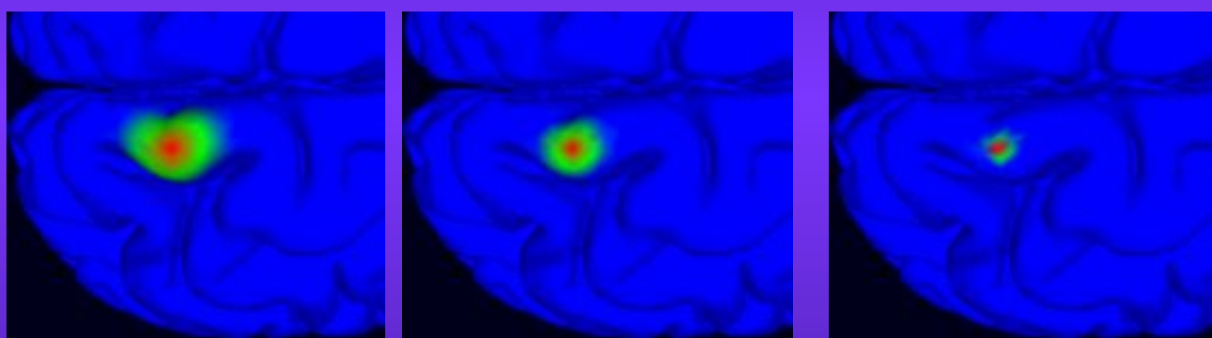

Inverse Problem
Equivalent current dipole

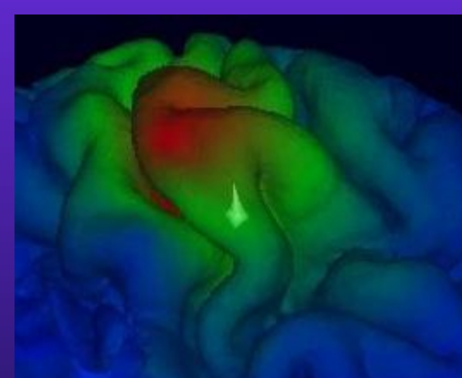

Source localization errors of patch activity

Head model: 4-layer MR-based BEM model

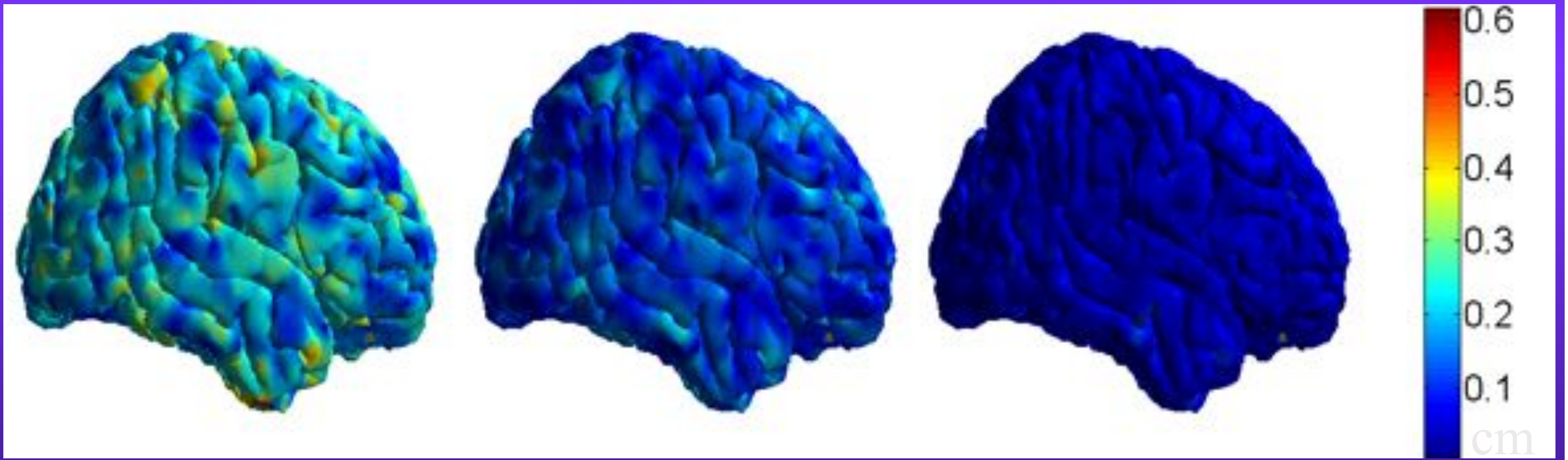

Patch size = 10 mm Patch size = 6 mm Patch size = 3 mm

Source localization errors of patch activity

Head model: 3-layer spheres

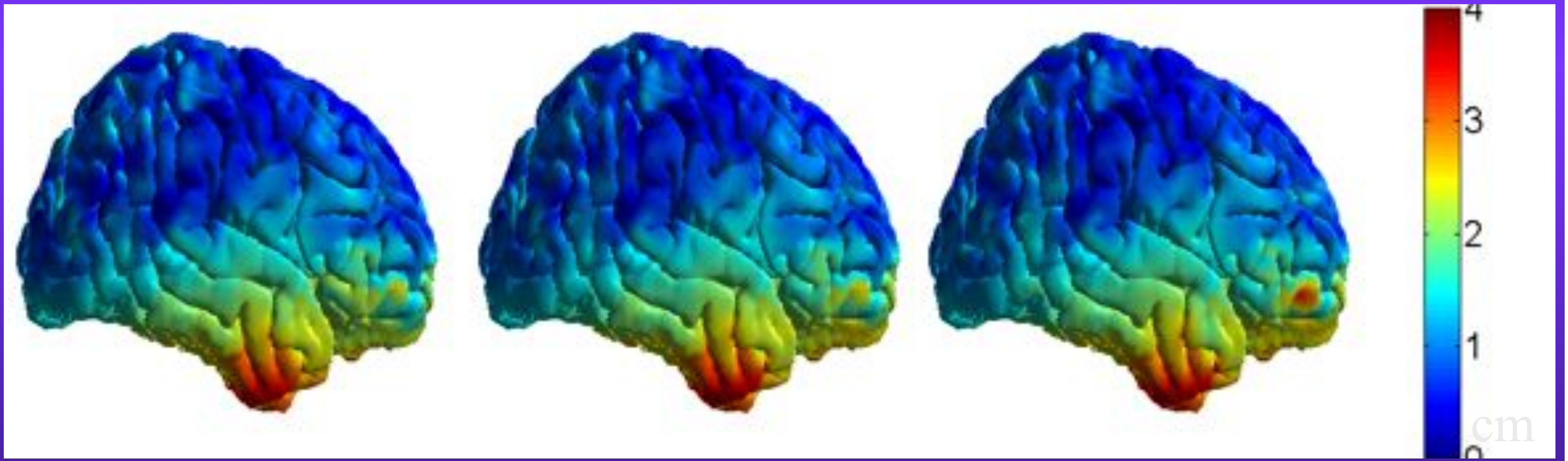

Patch size = 10 mm   Patch size = 6 mm   Patch size = 3 mm

Observations

- Spherical Model
  - Location errors more than 4 cm.
- 3-Layer MNI
  - Large errors where models do not agree.
  - Higher around chin and the neck regions.
- 4-Layer MNI
  - Similar to 3-Layer MNI.
  - Smaller in magnitude.

Electrode co-registration errors

- Solve FP with reference model
- Shift all electrodes and re-register
  - 5° backwards
  - 5° left
- Localize using shifted electrodes
- Plot location and orientation errors

5° Backwards Location Errors

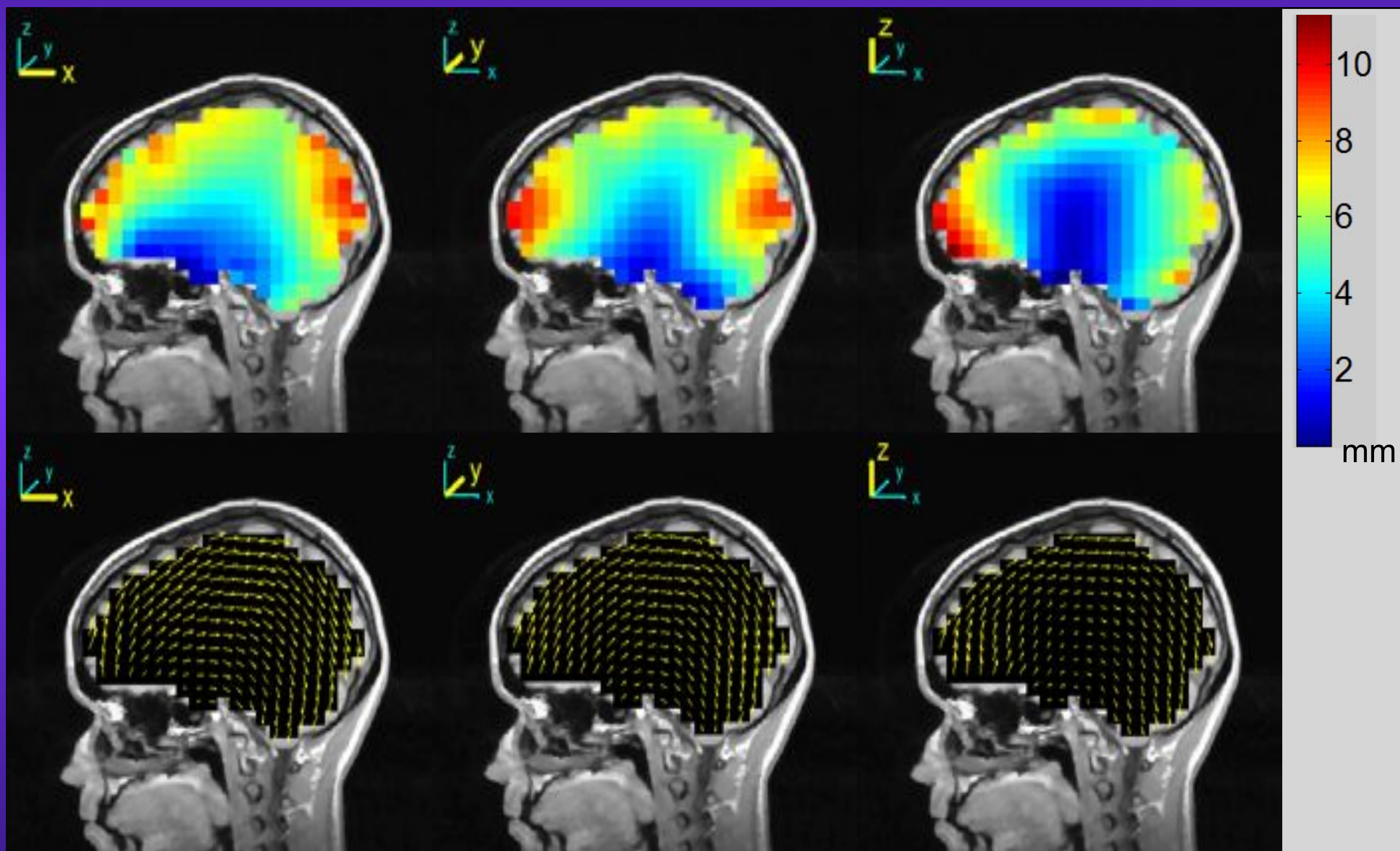

5° Left Location Errors

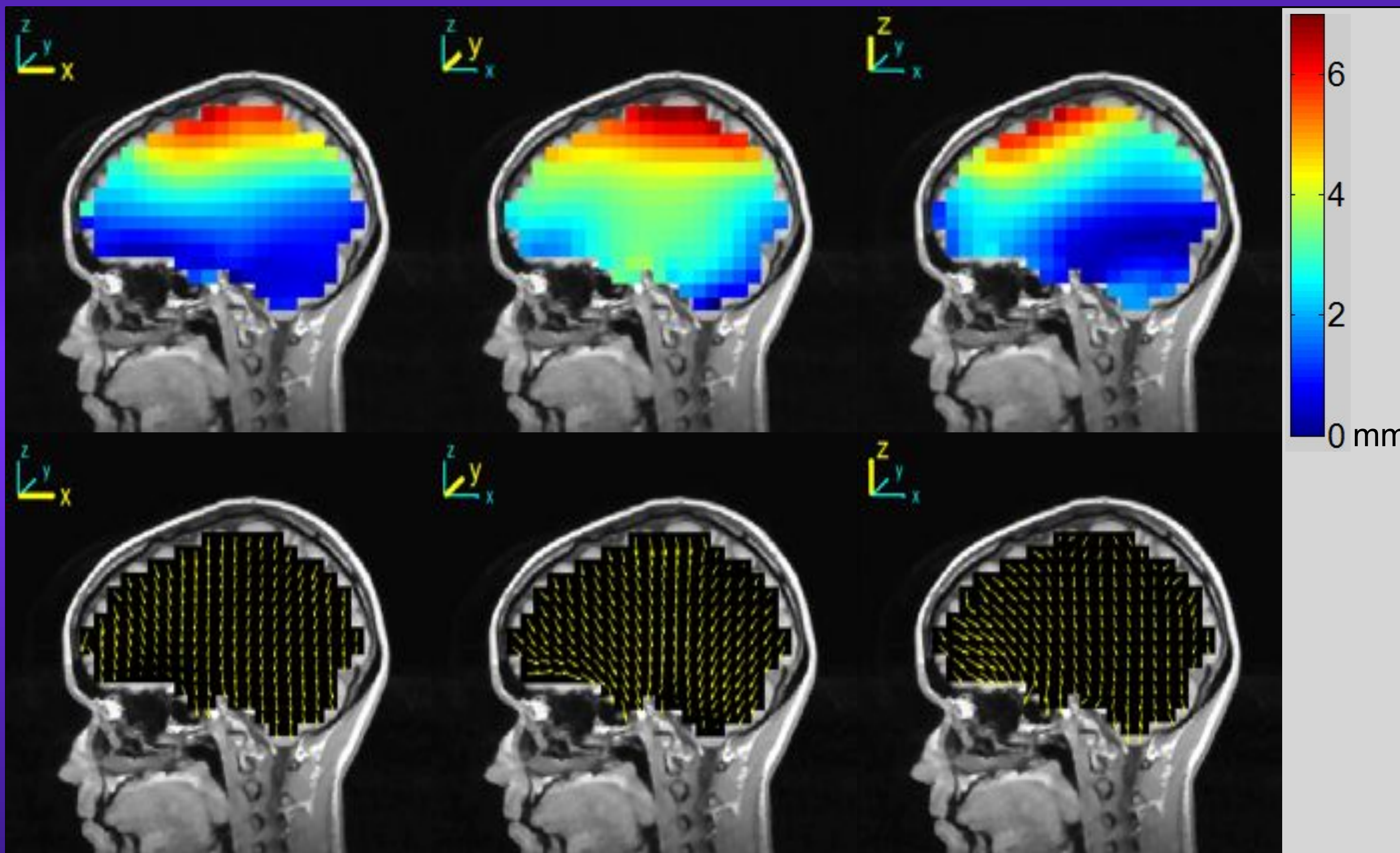

Observations

- Errors increase close to the surface near electrode locations.
- Changing or incorrectly registering electrodes may cause 5-10 mm localization error.

Effect of skull conductivity

Measurement of skull conductivity

MREIT
Magnetic stimulation
Current injection

In vivo

Hoekama et al, 2003

In vitro

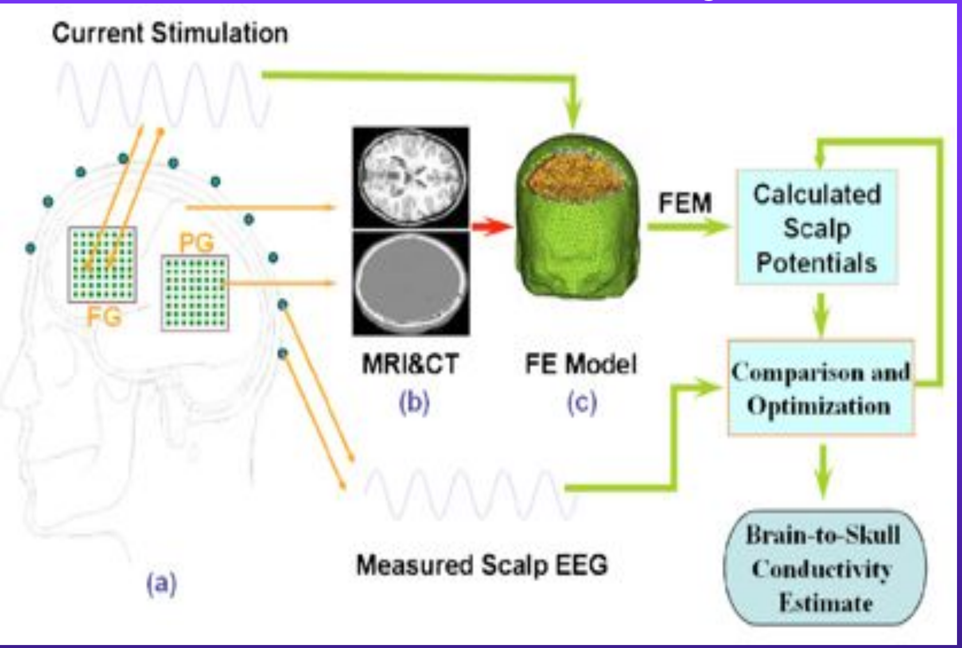

He et al, 2005

Effect of skull conductivity

Brain to skull ratio		
Rush and Driscoll	1968	80
Cohen and Cuffin	1983	80
Oostendorp et al	2000	15
Lai et al	2005	25

Measurement	Age	σ (mS/m)	Sd (mS/m)
Agar-agar phantom	–	43.6	3.1
Patient 1	11	80.1	5.5
Patient 2	25	71.2	8.3
Patient 3	36	53.7	4.3
Patient 4	46	34.4	2.3
Patient 5	50	32.0	4.5
Post mortem skull	68	21.4	1.3

Skull conductivity by age

Hoekama et al, 2003

Effect of Skull Conductivity

- Solve FP with reference model
  - Brain-to-Skull ratio: 80
- Generate test model
  - Same geometry
  - Brain-to-Skull ratio: 20
- Localize using test model
- Plot location and orientation errors

FP ratio: 80 IP ratio: 20

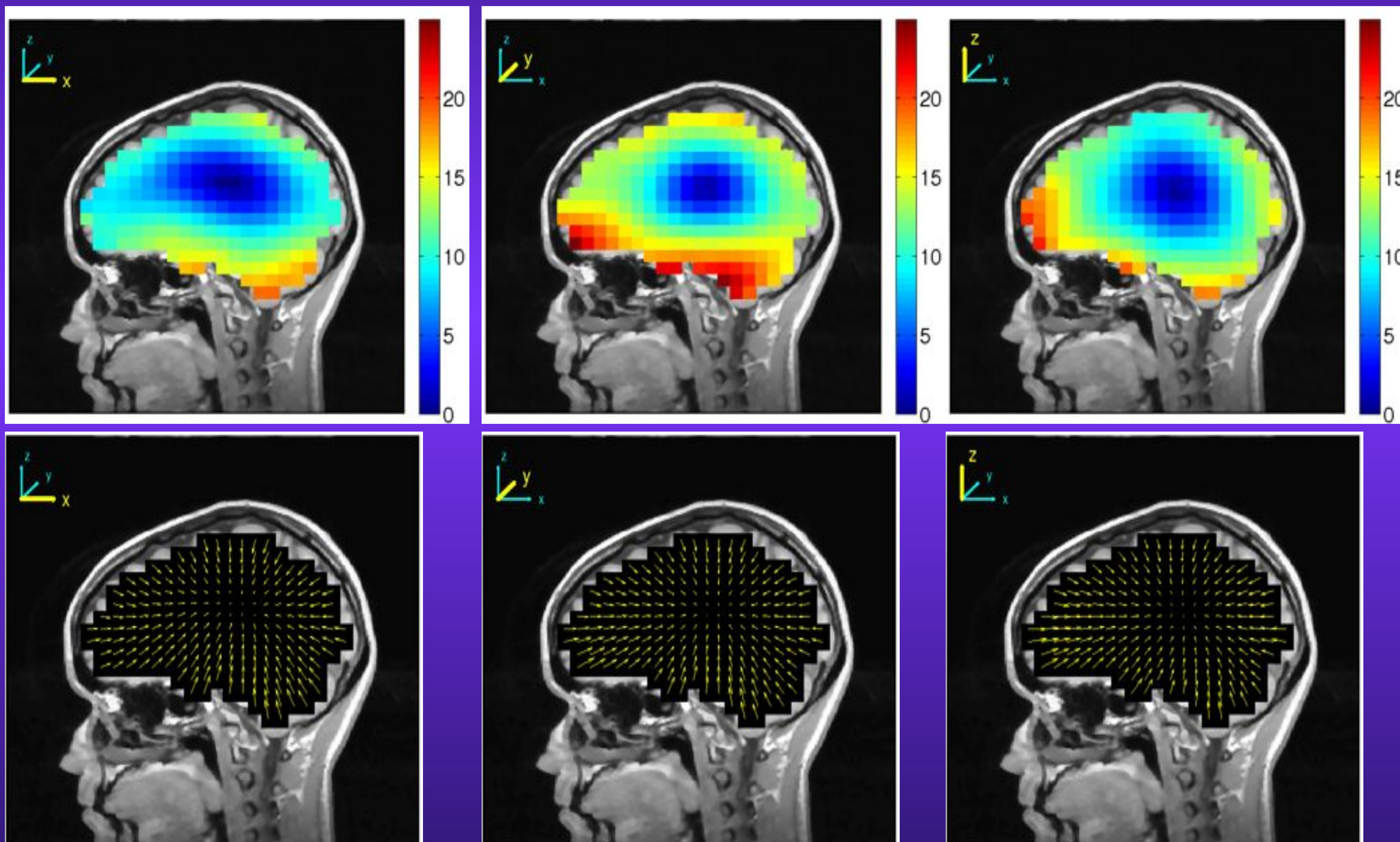

Conclusion

- Head shape
  - Most impact on source localization accuracy.
- Incorrect electrode registration
  - Errors near the electrodes
  - Most studies investigate cortical activity close to the electrodes.
- Electrical properties
  - Number of layers
  - Relative conductivities (Brain-to-Skull ratio)

Epilepsy Head Modeling

CASE STUDY

Epilepsy Head Modeling

- Large hole in skull
- Plastic sheet
- A pre-surgery MR and post-surgery CT
- Differences in brain shape after surgery
- Co-registration of electrodes
  - Subdural – from CT segmentation
  - Scalp – no digitizer data

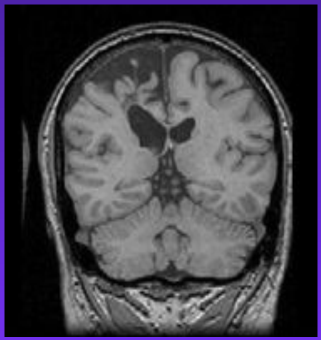

MR

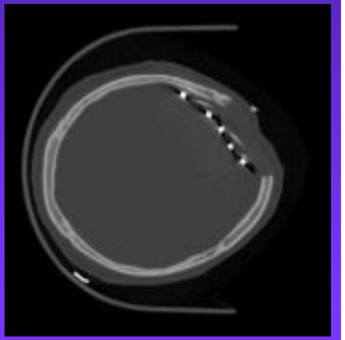

CT

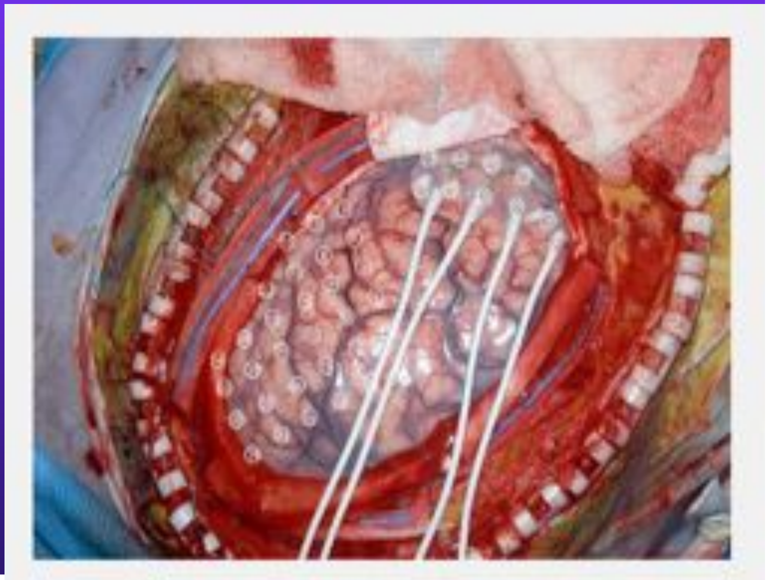

Head modeling in epilepsy

Pre-surgery MR
0.86 x 1.6 x 0.86 mm

Post-surgery CT
0.49 x 0.49 x 2.65 mm

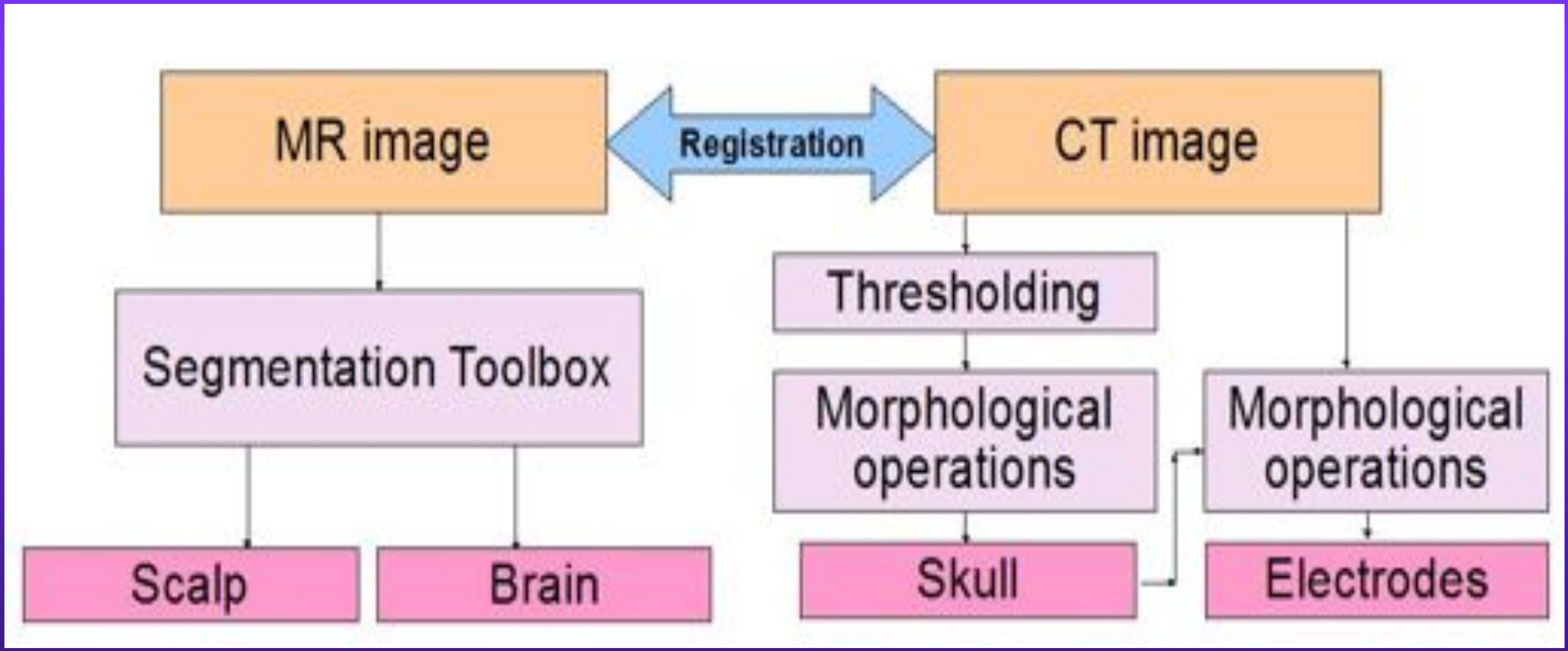

Scalp, skull and sheet models

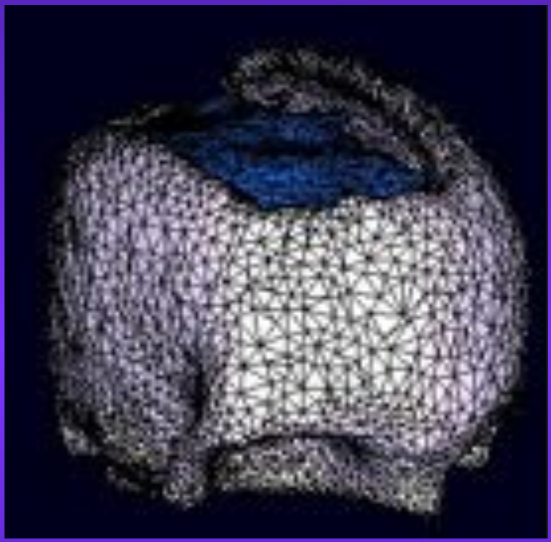

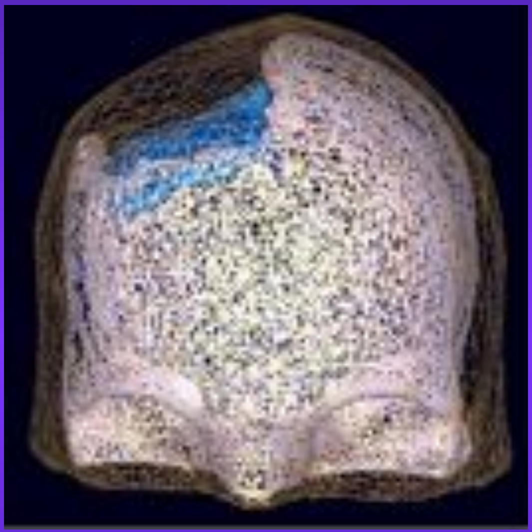

Number of elements:
Scalp: 10000
Skull: 30000
Plastic sheet : 7000

BEM model

Analyzing Epilepsy Recordings

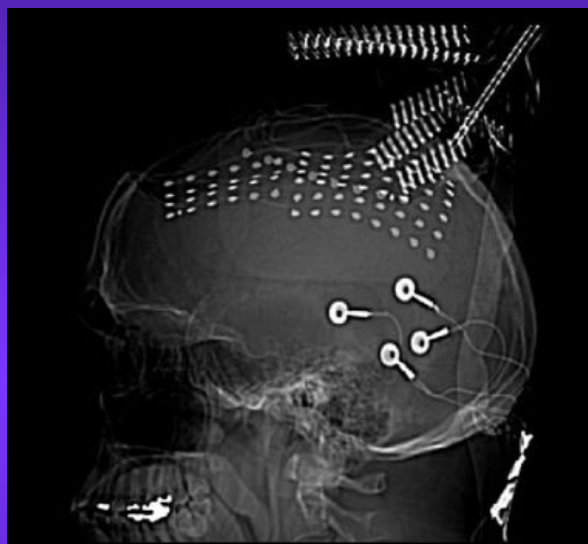

CT image of the implanted grid electrodes

- Pre-Surgical Evaluation
- Rest Data
- Simultaneous recordings
  - 78 iEEG electrodes
  - 29 scalp electrodes
- Provided by Dr. Greg Worrell, Mayo Clinic

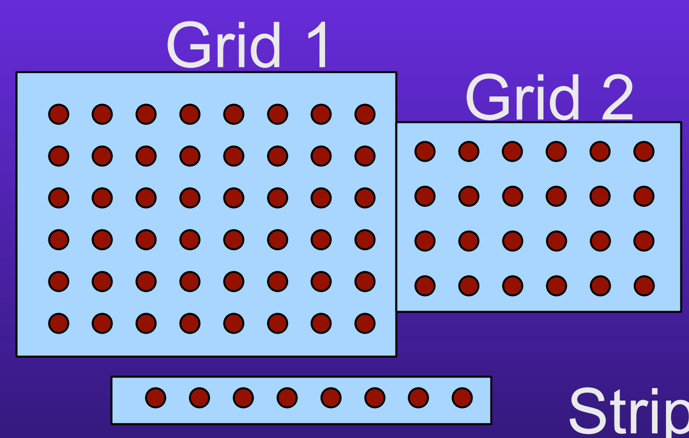

iEEG data

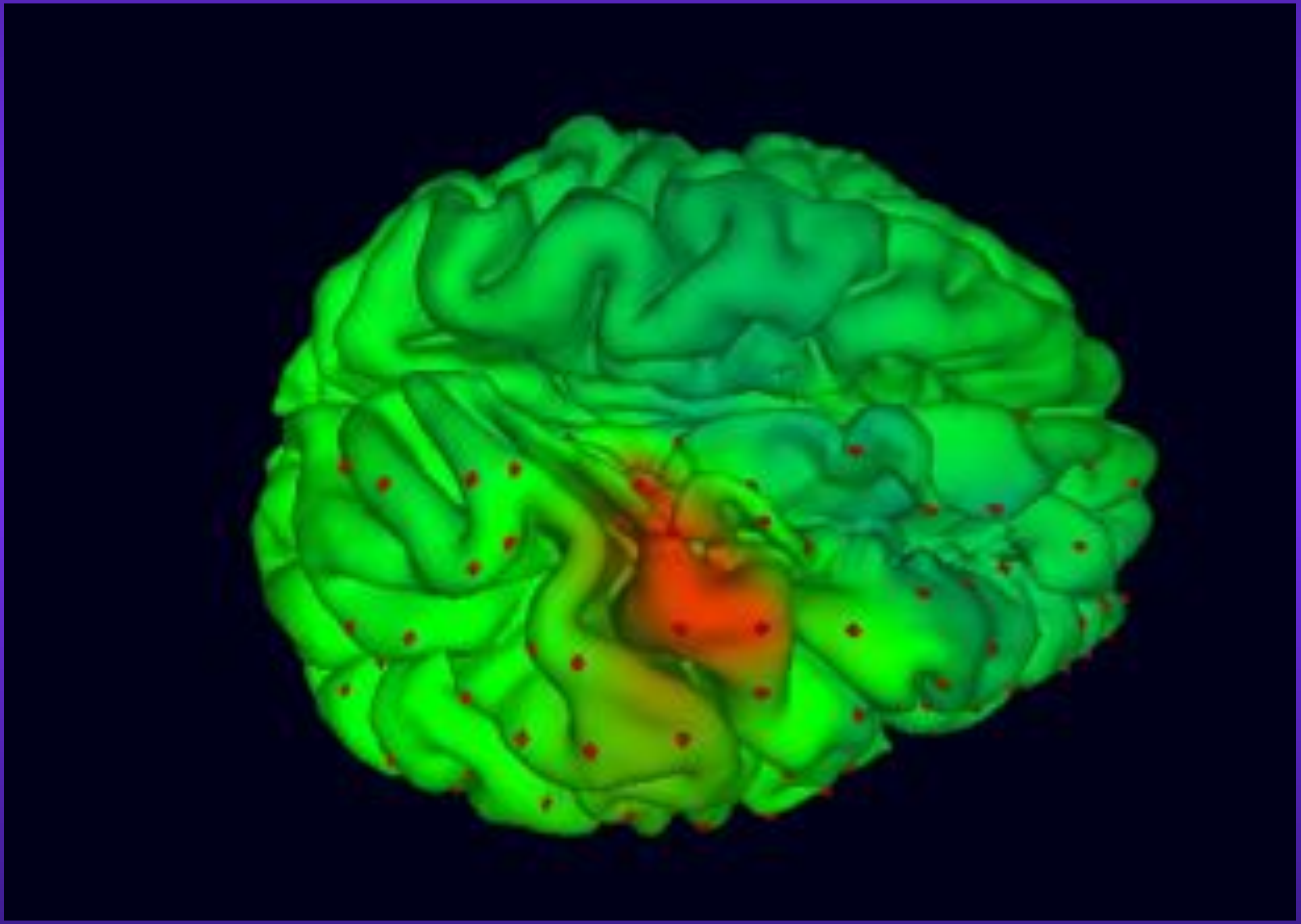

Independent Component Analysis

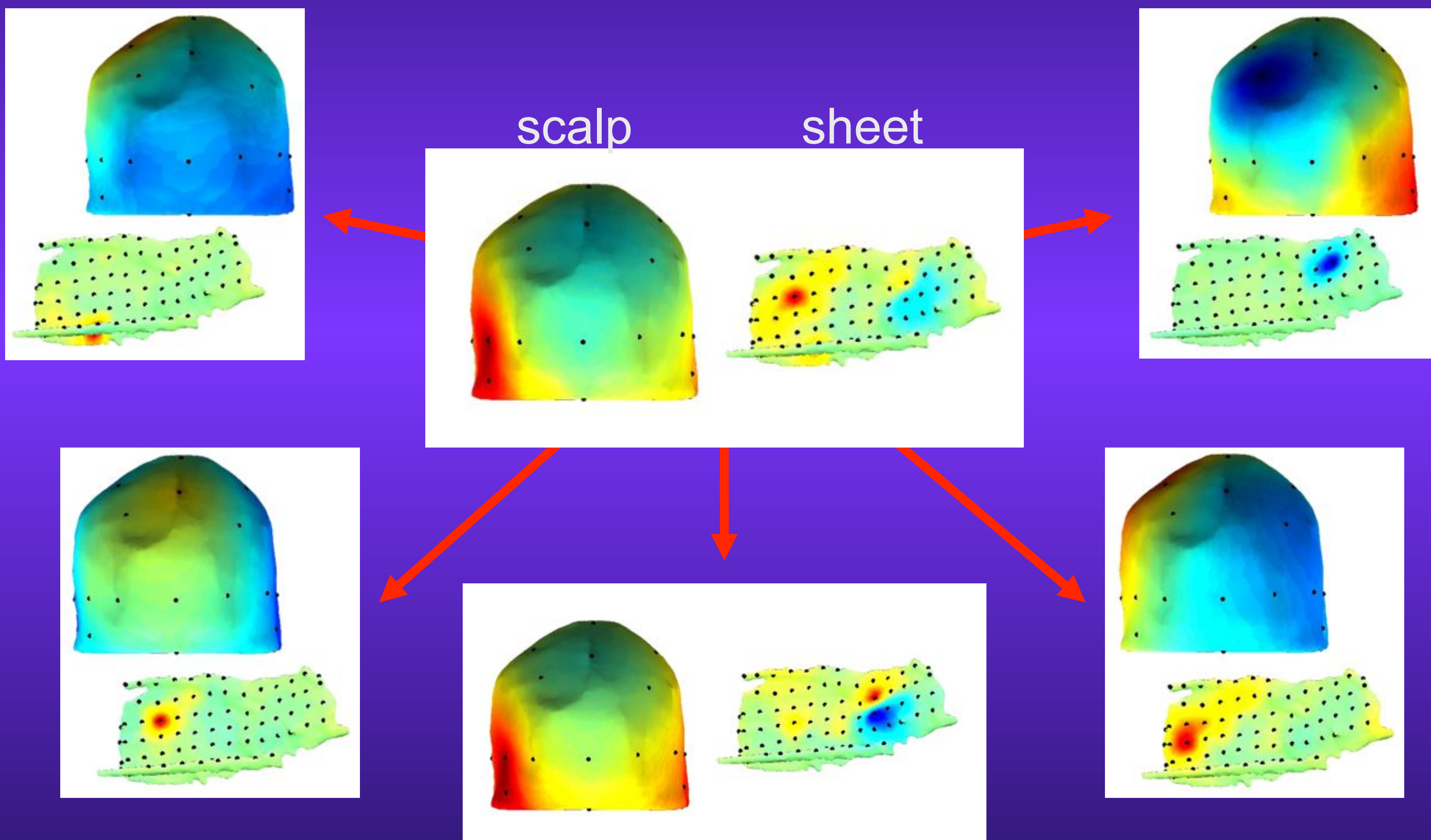

Independent Components

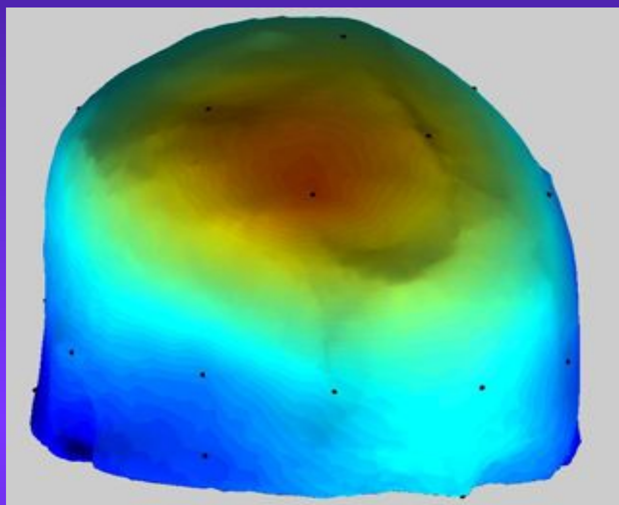

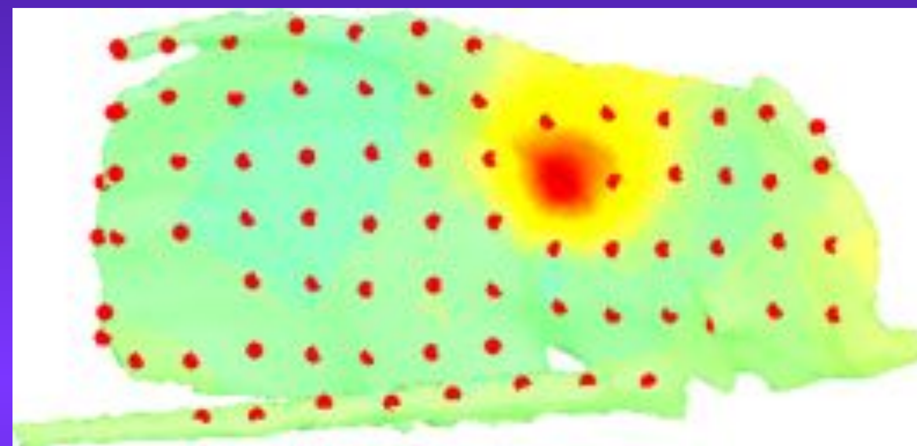

Potentials on scalp

Potentials on plastic sheet

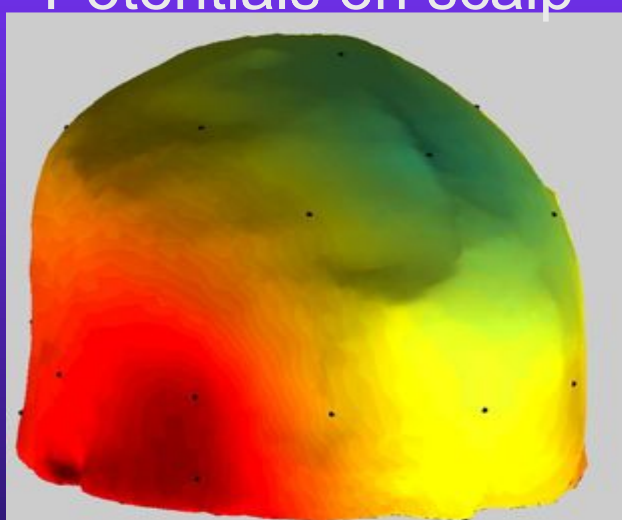

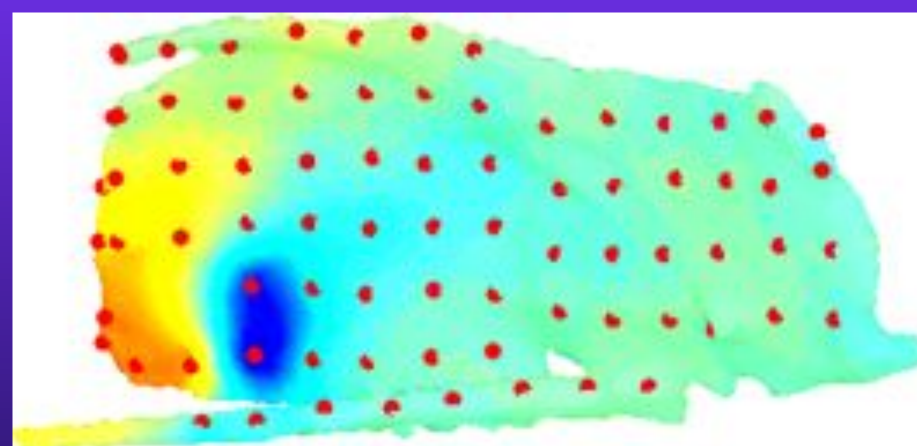

Independent Components on Brain Surface

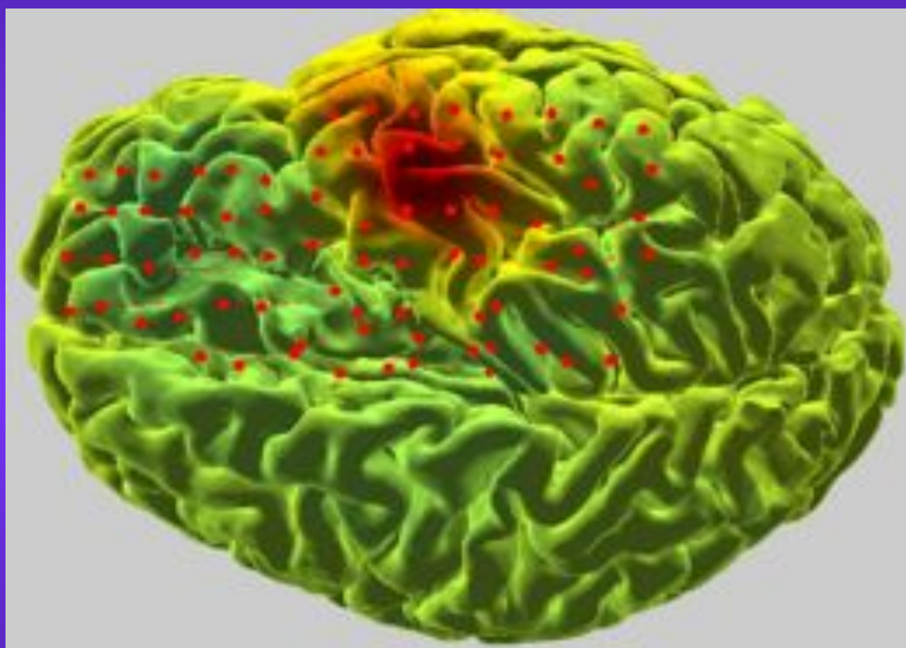

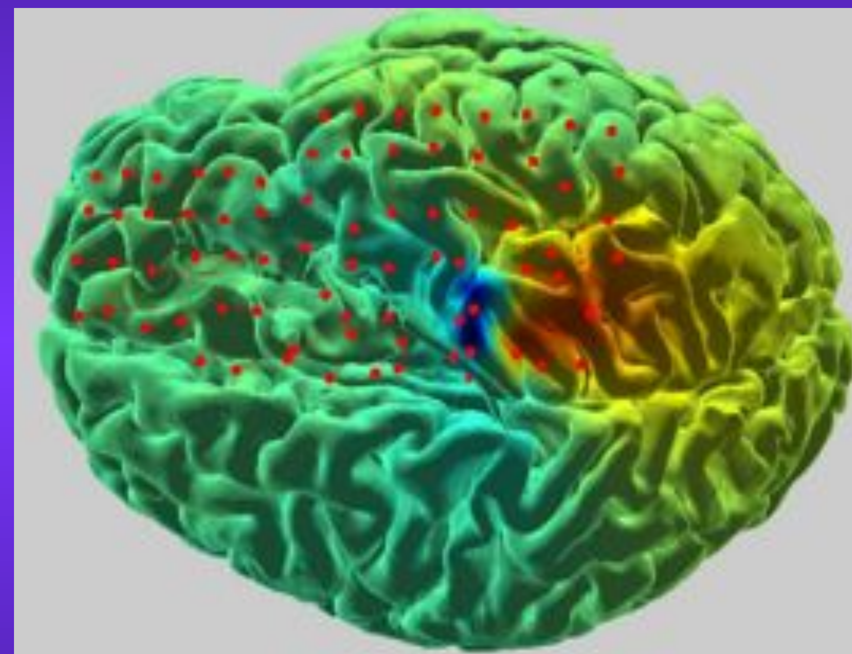

Source Localization Results

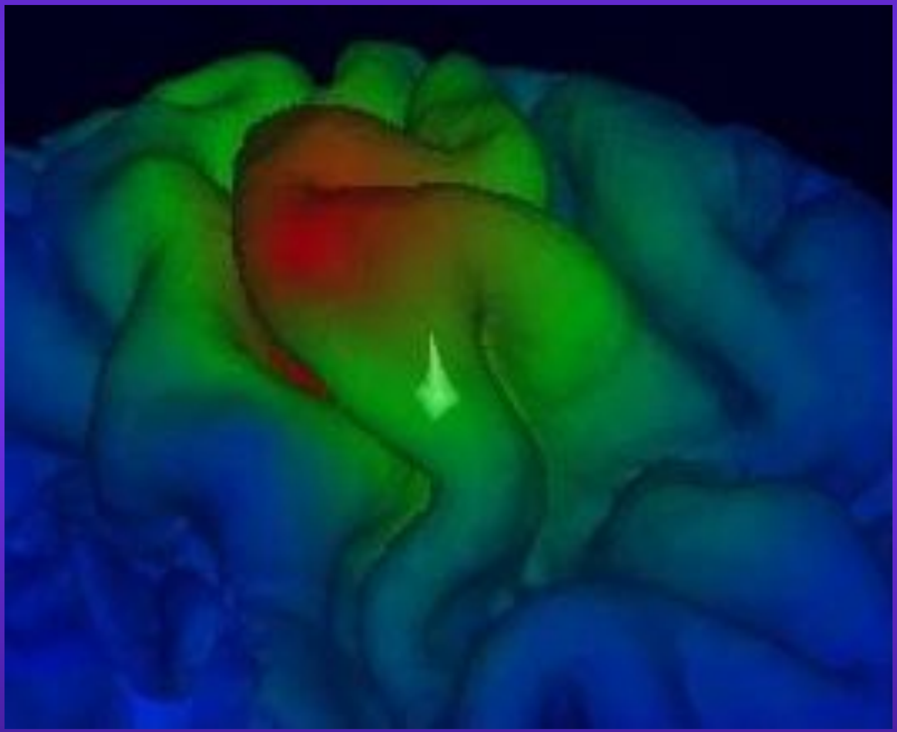

Radial source

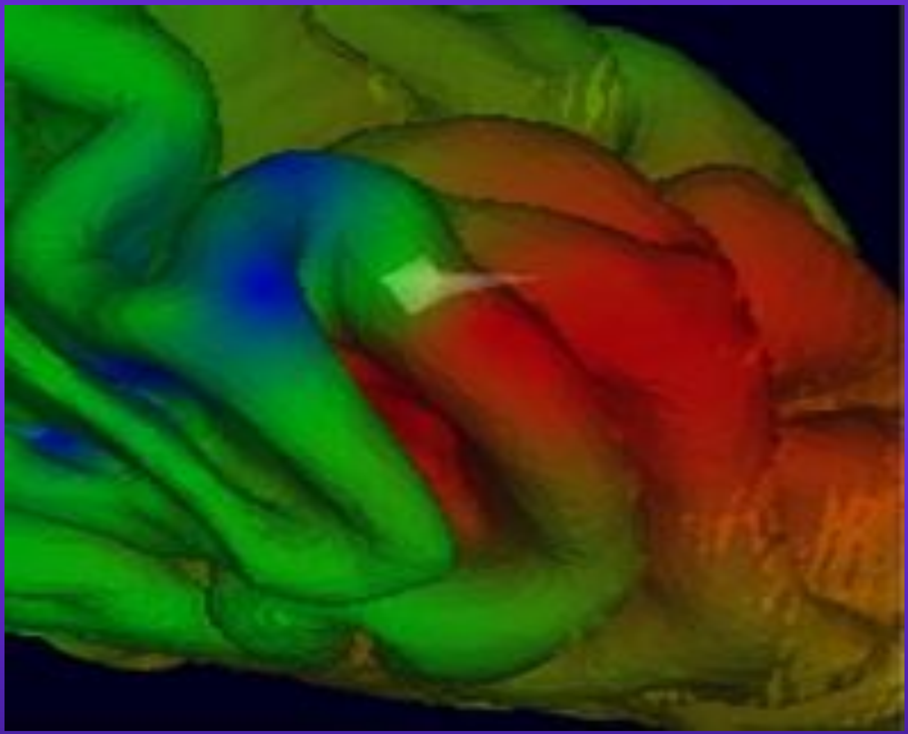

Tangential source

Distributed source localization

Patch - based source localization

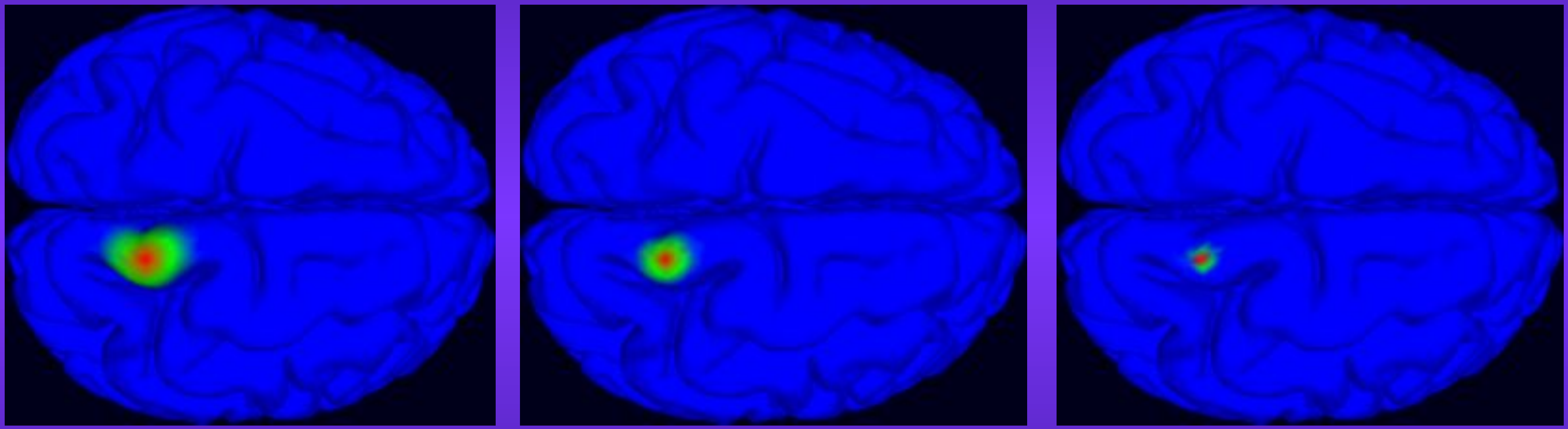

Three Gaussian patches in different scales with radius 10mm, 6mm, and 3mm.

Cortical activity

Cortical activity of the two IC maps

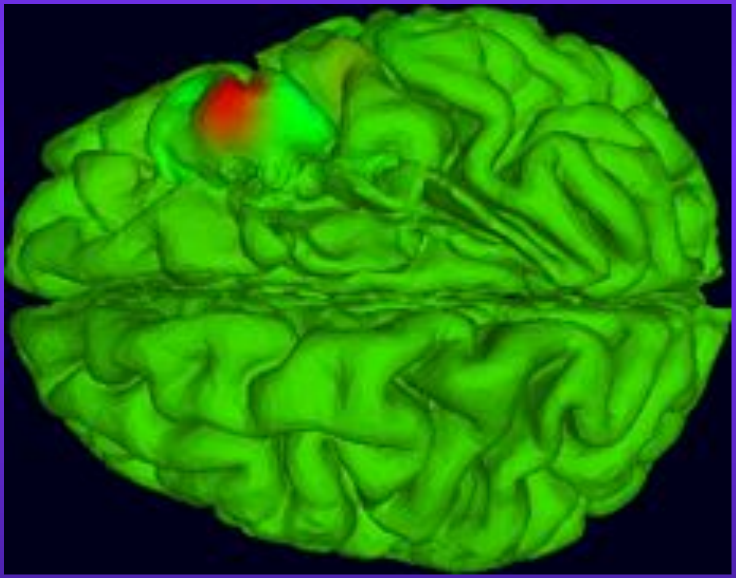

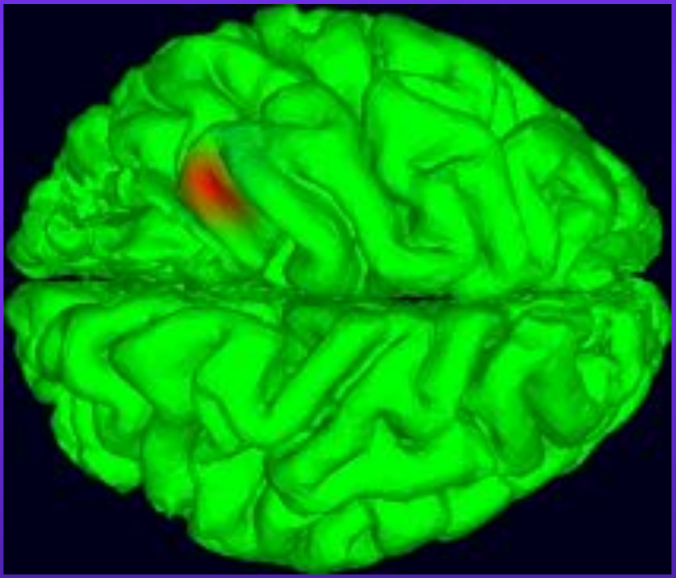

The SBL algorithm managed to identify sparse mixtures of overlapping patches that describe both components.

Cortical activity of seizure components

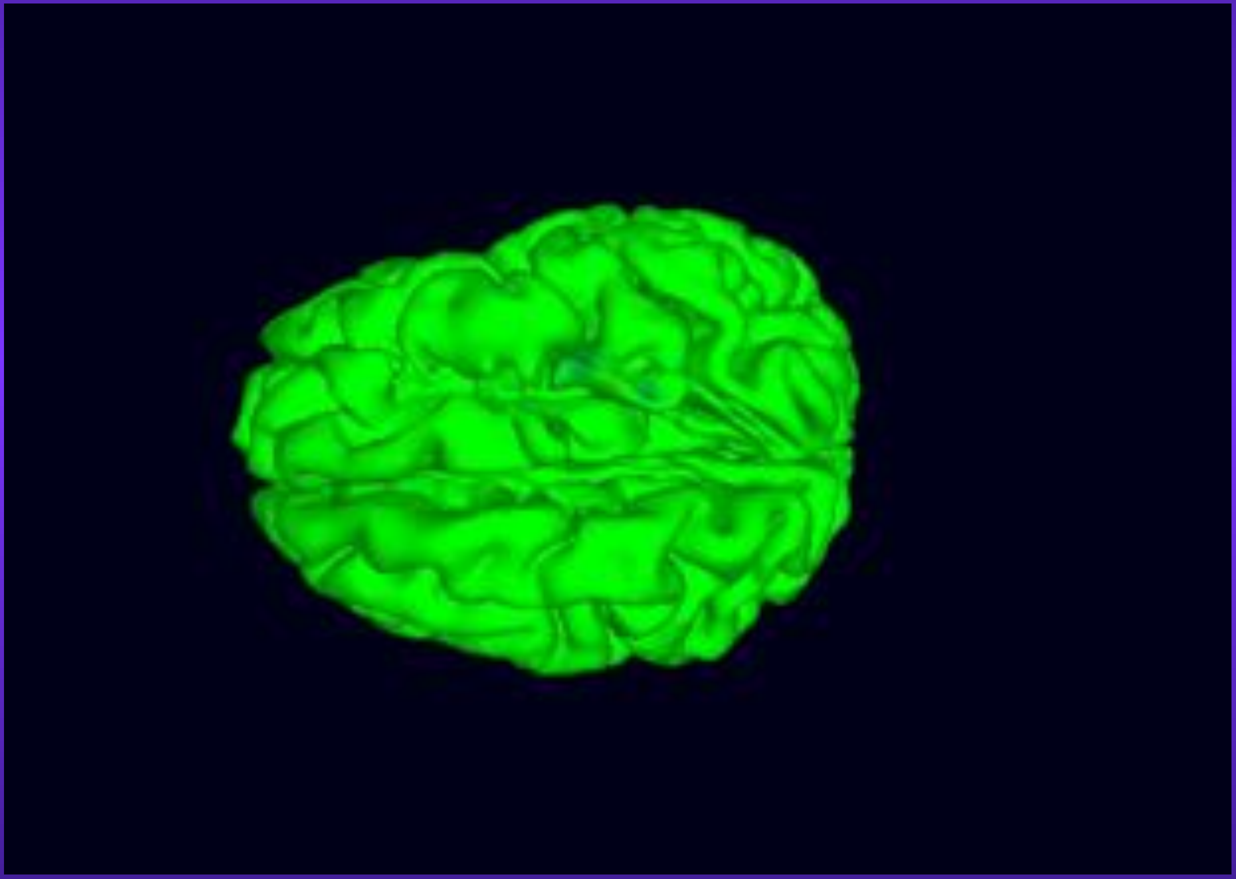

Final Words

- Accurate source localization
  - Realistic head models.
  - Correct electrode locations.
  - Signal Processing
- NFT can work with EEGLAB
  - Create realistic models

References

1. Z. Akalin Acar, S. Makeig, “Neuroelectromagnetic Forward Head modeling Toolbox”, J. of Neuroscience Methods, vol. 190 (2), 258-270, 2010.
2. Z. Akalin Acar, N. Gencer, “An advanced boundary element method (BEM) implementation for the forward problem of electromagnetic source imaging”, vol. 49, 5011-5028, 2004.
3. Z. Akalin Acar, G. Worrell, S. Makeig, “Patch-based cortical source localization in epilepsy”, Proc. of IEEE EMBC 2009, Minneapolis.
4. Z. Akalin Acar, S. Makeig, “Effect of head models in EEG source localization”, Sfn 2010, San Diego.